

# Lawrence Berkeley National Laboratory

## LBL Publications

### Title

Characterization of the Selective Reduction of NO by NH<sub>3</sub>

### Permalink

<https://escholarship.org/uc/item/4d6327cv>

### Authors

Brown, N J

Sawyer, R F

Lucas, D

### Publication Date

1981-07-01



# Lawrence Berkeley Laboratory

UNIVERSITY OF CALIFORNIA

## ENERGY & ENVIRONMENT DIVISION

Submitted to Combustion and Flame

CHARACTERIZATION OF THE SELECTIVE REDUCTION  
OF NO BY NH<sub>3</sub>

N.J. Brown, R.F. Sawyer, and D. Lucas

July 1981.

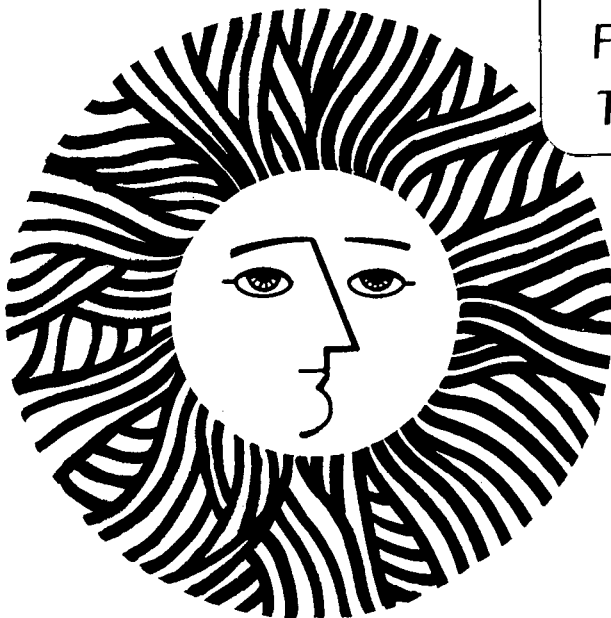
RECEIVED  
LAWRENCE  
BERKELEY LABORATORY

AUG 6

LIBRARY  
DOCUMENTS

### TWO-WEEK LOAN COPY

*This is a Library Circulating Copy  
which may be borrowed for two weeks.  
For a personal retention copy, call  
Tech. Info. División, Ext. 6782*



LBL-12549  
c. 2

## **DISCLAIMER**

This document was prepared as an account of work sponsored by the United States Government. While this document is believed to contain correct information, neither the United States Government nor any agency thereof, nor the Regents of the University of California, nor any of their employees, makes any warranty, express or implied, or assumes any legal responsibility for the accuracy, completeness, or usefulness of any information, apparatus, product, or process disclosed, or represents that its use would not infringe privately owned rights. Reference herein to any specific commercial product, process, or service by its trade name, trademark, manufacturer, or otherwise, does not necessarily constitute or imply its endorsement, recommendation, or favoring by the United States Government or any agency thereof, or the Regents of the University of California. The views and opinions of authors expressed herein do not necessarily state or reflect those of the United States Government or any agency thereof or the Regents of the University of California.

CHARACTERIZATION OF THE SELECTIVE REDUCTION OF NO BY NH<sub>3</sub>

N.J. Brown and R.F. Sawyer  
Principal Investigators

and

D. Lucas  
Staff Scientist

Energy and Environment Division  
Lawrence Berkeley Laboratory  
University of California  
Berkeley, California 94720

This work was supported by the U.S. Department of Energy under Contract Number W-7405-ENG-48; Report submitted to the State of California Air Resources Board for the grant period July 20, 1979 to January 31, 1981, Contract #A8-146-31.

ABSTRACT

The selective reduction of NO by NH<sub>3</sub> addition has been studied in a lean-burning oil fired laboratory combustion tunnel as a function of equivalence ratio, NH<sub>3</sub> injection temperature, concentration of NH<sub>3</sub> added, and the source of NO. Ammonia breakthrough was found to depend strongly on the NH<sub>3</sub> addition temperature. The total concentration of nitrogen containing species other than N<sub>2</sub>, NO, and NH<sub>3</sub> was measured with a variety of techniques and was found to be less than 5 ppm over the range of conditions studied.

## EXECUTIVE SUMMARY

In recognition that the selective reduction of NO through the addition of  $\text{NH}_3$  to post combustion gases containing excess air now appears to be a viable control process for stationary source combustion, this research has been directed toward characterizing Thermal  $\text{DeNO}_x$  for oil fuels. The research has been divided into five tasks which are discussed briefly in this summary and in detail in our report.

The first task involved modification of the previously constructed combustion tunnel to enable us to burn liquid fuels as sprays in a reproducible, steady state manner. The combustion tunnel consists of a combustion section, an ammonia injection region, and a reaction and sampling section. Diesel oil is delivered to a Monarch high pressure atomizing oil burner nozzle. Rapid mixing and burning of the fuel/air mixture is enhanced by several fixed disks located behind the fuel nozzle. A 10 cm diameter section of steel tubing is installed immediately downstream of the fuel nozzle to increase the residence time of reactants in the flame region. The temperature of the combustion products leaving the first section is adjusted by watercooling the tunnel wall. Ammonia injection is accomplished with four quartz injectors which are carefully placed to achieve complete mixing of the ammonia. The reaction and sampling system begins immediately downstream of the ammonia injection position and is approximately 60 cm long. Temperature and composition sampling is performed at four axial locations separated by 12 cm.

Meaningful experimental results can be obtained when combustor performance is steady state over the duration of a given experiment and reproducible on a day-to-day basis. A series of experiments which determined

completeness of combustion, the mixing of combustion products and uniformity of the temperature field in the reaction section were performed over the range of conditions employed in our characterization studies. The results of these experiments assured us that the condition in the reaction section where the selective reduction occurs could be well controlled. The results of these experiments are documented in part III of the report.

The second task involved the development of analytical techniques to identify nitrogen containing products of the selective reduction. Sample extraction is accomplished with quartz microprobes. Measurement of NO, CO and CO<sub>2</sub> is accomplished routinely with commercial instrumentation which has been carefully calibrated. Water concentrations are determined by metering flows of products gases into pre-weighed magnesium perchlorate drying tubes and determining the water vapor collected by weighing. Three highly precise and accurate analytical techniques have been developed to measure NH<sub>3</sub> in combustion exhausts. The sodium phenolate method, a wet chemical colorimetric method, has been refined for combustion applications and is our standard for other methods. Ammonia measurements are also made with a chemiluminescent analyzer, modified to prevent condensation. Conversion efficiency has been demonstrated to be independent of NH<sub>3</sub> concentration. Random ammonia measurements made by the chemiluminescent technique are checked with the sodium phenolate method for verification of accuracy and to demonstrate the absence of other nitrogenous species. Ammonia measurements are also performed with gas permeable specific ion electrodes (Orion Model 95-10). Three techniques are also utilized for the detection of and quantification of hydrogen cyanide. The simplest employed a Matheson Kitagawa detector tube kit, and a second method utilized a gas permeable specific ion electrode. A Varian 3700 gas chromatograph

equipped with a flame ionization detector is also used for hydrogen cyanide and nitrile detection. A Hewlett-Packard 5750 gas chromatograph with thermal conductivity and flame ionization detectors is employed to measure  $N_2$ ,  $O_2$ , CO,  $CO_2$  and hydrocarbons. Sulfur dioxide is measured with a commercial fluorescent analyzer.

The third task involved investigating the selective reduction of NO by  $NH_3$  under a variety of experimental conditions. The reduction is investigated at several equivalence ratios, for several  $NH_3$  addition temperatures and for several  $NH_3$  concentrations. Fuel nitrogen is simulated by the addition of NO prior to combustion or by adding fixed quantities of pyridine to the diesel oil. Fuel sulfur concentration is fixed by the addition of known quantities of thiophene. Results are expressed in terms of terminal NO and  $NH_3$  concentrations. Exhaust gases are also analyzed for CO,  $CO_2$ ,  $SO_2$ , hydrocarbons and other nitrogenous species.

One result common to all prototype fuels is as more ammonia is injected, more NO reduction occurs and more  $NH_3$  breakthrough occurs. The reduction process shows a dependence on both the ammonia concentration and equivalence ratio. At a fixed equivalence ratio, the optimum reduction temperature increases with increasing  $\beta$ . At high equivalence ratios (close to stoichiometric), this trend is less obvious and becomes more apparent at leaner conditions. The range for optimum reduction temperature varies from 1150 to values in excess of 1250K. The fraction of NO reduced does not vary significantly with equivalence ratio as long as excess oxygen is present. Ammonia breakthrough is strongly dependent upon temperature and is dependent upon initial  $NH_3$  concentration for temperature conditions when breakthrough is important. Ammonia breakthrough is independent of equivalence ratio for the range of equivalence ratios considered.



One of the most important results of this study is the absence of appreciable concentrations of nitrogenous species other than  $N_2$ ,  $NO$ ,  $NO_2$ , and  $NH_3$  when the reduction occurs under lean conditions. A conservative upper limit for the total concentration of these "odd nitrogen" species is 5 ppm. We set this limit based on the absence of compounds measured directly by techniques such as GC, GC/MS, and wet chemical methods which are sensitive to nitrogenous compounds, and the agreement between the different analytical techniques used to measure  $NO$ ,  $NO_x$ , and  $NH_3$ . As the different methods employed have widely different interferences, an appreciable concentration of an unobserved "odd nitrogen" compound could be detected as a difference in the measured concentration of  $NO_x$  or  $NH_3$ . Nitrogen compounds that are most certainly absent include HCN, nitriles, and amines. The carbon skeleton of nitriles or amines would have been detected by the flame ionization detector. The absence of hydrocarbons or  $H_2$  in the exhaust gases corroborates these results. The compound  $N_2O$  is not detectable in the chemiluminescent detector. Nitrous oxide is separable on Poropak Q but was not detected; however, we did not establish the sensitivity of the thermal conductivity detector to  $N_2O$ .

The presence of fuel sulfur has a definite effect upon Thermal De $NO_x$ , and our results are the first to investigate this systematically. The presence of fuel sulfur has two different, though interrelated manifestations: there is an increase in the conversion of fuel nitrogen to  $NO$  as the fuel is burned, and the optimum temperature for the  $NH_3$  reduction process shifts to higher values. Both effects vary directly with initial thiophene concentration. Sulfur compounds in the post combustion gases could affect the reduction process by reacting with the ammonia or an ammonia derived

species, effectively lowering the concentration of the reducing agent (lower  $\beta$ ). This would result in less NO reduction and in a decrease in the temperature for achieving the optimum NO reduction. Neither of these is observed. Lower concentration of  $\text{SO}_2$  and  $\text{NH}_3$  are measured when both species are present, but this is most likely attributable to reactions in the sampling system. The observed shift in the optimum temperature suggests a change in the reaction mechanism, or the presence of a competing reaction pathway when sulfur compounds are present. Sulfur dioxide has been identified as the major product of sulfur compounds in lean combustion environments; however, other sulfur compounds present in significantly smaller concentrations could play a role in the nitrogen/sulfur chemistry.

A fourth task in our research involved maintaining contact with investigators at the Statewide Air Pollution Research Center at Riverside. This has been accomplished. A continuing assessment of the scientific literature pertinent to Thermal  $\text{DeNO}_x$  has been maintained, as the fifth task in our research effort. A brief summary of the major findings of current research is given in the report. The report is concluded with a discussion of the implication of our own findings on full scale utility applications of Thermal  $\text{DeNO}_x$ .

TABLE OF CONTENTS

	<u>Page</u>
ABSTRACT . . . . .	1
EXECUTIVE SUMMARY . . . . .	2
TABLE OF CONTENTS . . . . .	7
LIST OF FIGURES . . . . .	8
LIST OF TABLES . . . . .	10
ACKNOWLEDGEMENT . . . . .	11
I. INTRODUCTION . . . . .	12
A. Selective Reduction Studies . . . . .	13
II. DESCRIPTION OF THE EXPERIMENT . . . . .	17
A. Experimental Apparatus . . . . .	17
B. Analytical Techniques . . . . .	22
C. Species Analysis . . . . .	24
III. SYSTEM CHARACTERIZATION . . . . .	37
A. NH <sub>3</sub> Mixing Characterization . . . . .	42
B. Reduction of NO by NH <sub>3</sub> . . . . .	43
IV. RESULTS . . . . .	49
A. Fuel Nitrogen: NO . . . . .	49
B. Fuel Nitrogen: Pyridine . . . . .	59
C. Fuel Nitrogen: Pyridine; Fuel Sulfur: Thiophene . . . . .	67
V. DISCUSSION . . . . .	74
VI. SIGNIFICANCE TO LARGE SCALE APPLICATIONS . . . . .	79
LIST OF REFERENCES . . . . .	83
LIST OF ABBREVIATIONS AND SYMBOLS . . . . .	85

LIST OF FIGURES

	<u>Page</u>
Figure 1. Schematic diagram of the laboratory scale combustion tunnel . . . . .	18
Figure 2. Schematic diagram of the NH <sub>3</sub> injectors . . . . .	21
Figure 3. Radiation correction for Chromel-Alumel thermocouple determined by suction pyrometry . . . . .	23
Figure 4. Schematic diagram of the ammonia collection system for the sodium phenolate method . . . . .	26
Figure 5. Conversion of NH <sub>3</sub> to NO as a function of converter temperature at a constant NH <sub>3</sub> concentration of 1000 ppm . . . . .	29
Figure 6. Conversion of NH <sub>3</sub> to NO as a function of NH <sub>3</sub> concentration at a constant converter temperature of 1190K . . . . .	30
Figure 7. Combustion effluent temperature measured along the combustor test section centerline for three different equivalence ratios . . . . .	38
Figure 8. Combustion effluent temperature measured as a function of radial distance at probe position B, 33 cm downstream of the NH <sub>3</sub> injectors, for $\phi = 0.89$ and flow velocities of a) 17 m/s and b) 21 m/s . . . . .	39
Figure 9. Concentration of NO measured as a function of axial position for the NH <sub>3</sub> reduction at $\phi = 0.83$ , $T^* = 1224K$ , and various $\beta$ values . . . . .	47
Figure 10. Concentration of NH <sub>3</sub> measured as a function of axial position for the NH <sub>3</sub> reduction at $\phi = 0.83$ , $T^* = 1224K$ , and various $\beta$ values . . . . .	48
Figure 11. Concentration of NO and NH <sub>3</sub> measured centerline at probe position D as a function of $\beta$ for $\phi = 0.83$ and $T^* = 1120K$ . . . . .	50
Figure 12. The NO survival as a function of $\beta$ and $T^*$ for $\phi = 0.83$ with NO as the fuel nitrogen . . . . .	52
Figure 13. The NO survival as a function of $\beta$ and $T^*$ for $\phi = 0.89$ with NO as the fuel nitrogen . . . . .	53

	<u>Page</u>
Figure 14. The NO survival as a function of $\beta$ and $T^*$ for $\phi = 0.95$ with NO as the fuel nitrogen . . . . .	54
Figure 15. The NH <sub>3</sub> breakthrough measured at probe position D as a function of $\beta$ and $T^*$ for $\phi = 0.83$ . . . . .	55
Figure 16. The NH <sub>3</sub> breakthrough measured as a function of $\beta$ and $T^*$ for three equivalence ratios . . . . .	57
Figure 17. The NO survival as a function of $\beta$ and $T^*$ for $\phi = 0.78$ with pyridine as the fuel nitrogen (1.02% N) . . . . .	62
Figure 18. The NO survival as a function of $\beta$ and $T^*$ for $\phi = 0.89$ with pyridine as the fuel nitrogen (1.02% N) . . . . .	63
Figure 19. The NO survival as a function of $\beta$ and $T^*$ for $\phi = 0.94$ with pyridine as the fuel nitrogen (1.02% N) . . . . .	64
Figure 20. The NH <sub>3</sub> breakthrough measured as a function of $T^*$ for three different equivalence ratios at $\beta = 4.2 - 4.4$ . . . . .	65
Figure 21. The NO survival as a function of $\beta$ and $T^*$ for $\phi = 0.89$ with pyridine as the fuel nitrogen (1.02% N) and thiophene as the fuel sulfur (0.33% S) . . . . .	70
Figure 22. The NO survival as a function of $\beta$ and $T^*$ for $\phi = 0.89$ with pyridine as the fuel nitrogen (1.02% N) and thiophene as the fuel sulfur (0.63% S) . . . . .	71
Figure 23. The NO survival as a function of $\beta$ and fuel sulfur concentration for $\phi = 0.89$ and $T^* = 1175 - 1185$ K . . . . .	72

LIST OF TABLES

	<u>Page</u>
Table I. Measurements of NH <sub>3</sub> under cold flow conditions. . . . .	31
Table II. Measurements of NH <sub>3</sub> under combustion conditions . . . . .	32
Table III. Concentration of CO <sub>2</sub> measured at various probe positions. .	41
Table IV. Ammonia injection system mixing characteristics for T* = 1220 K and $\phi = 0.89$ . . . . .	44
Table V. Conversion of pyridine to NO for various T* values at three equivalence ratios . . . . .	60
Table VI. Conversion of pyridine to NO as a function of fuel sulfur added as thiophene for various T* values at $\phi = 0.89$ . . . .	68

ACKNOWLEDGEMENT

We are grateful to Dr. A.S. Newton for advice and assistance in development of analytical techniques, and to K.C. Metchette, who performed many of the measurements. The efforts and technical assistance of Dr. K.S. Basden, R.H. Jensen, T.S. Eitzen, and W.J. Pitz are greatly appreciated.

This work was supported by the U.S. Department of Energy under Contract Number W-7405-ENG-48; and submitted to the State of California Air Resources Board for the grant period July 20, 1979 to January 31, 1981, contract #A8-146-31.

## I. INTRODUCTION

More intensive regulations of the emissions of nitrogen oxides from stationary combustion sources have prompted the innovation and characterization of new control technologies suitable for applications in utilities. Previously employed technologies were largely based upon the prevention of thermal NO formation, and these are often ineffective in preventing the formation of fuel NO since the two mechanisms depend differently on experimental combustion conditions.

One of the more recent and attractive abatement technologies is the Exxon Thermal DeNO<sub>x</sub><sup>1</sup> described by Lyon and Longwell.<sup>2</sup> This process is based upon a reaction sequence between O<sub>2</sub>, NO, and NH<sub>3</sub>. This sequence can be utilized to reduce NO selectively in the post combustion environment containing excess O<sub>2</sub> following NH<sub>3</sub> addition at a specified temperature. This process has the advantage of allowing for the destruction of NO after its formation, and thus makes no distinction between thermal and fuel NO.

Characterization of the selective reduction of NO through reaction with NH<sub>3</sub>, added to the post combustion environment of lean mixtures, has involved different types of investigations which provide complementary information. Kinetic studies have been undertaken in a quartz flow reactor by Lyon and co-workers<sup>3-5</sup> to elucidate mechanistic details of the NH<sub>3</sub>/NO/O<sub>2</sub> reactions. Muzio et al.<sup>6-7</sup> investigated the selective reduction process for natural gas, a light oil and several types of coal, and have provided some mechanistic information and determined optimum conditions for maximizing the reduction of NO. Recent kinetic modelling studies have been undertaken by Saliman and Hanson<sup>8</sup> and by Miller et al.<sup>9</sup> to



investigate whether existing kinetic data are adequate for providing explanations of the features of the selective reduction determined experimentally. Although each of these studies has increased our understanding of the chemistry associated with Thermal DeNO<sub>x</sub> and given us an appreciation of the process sensitivity to operating conditions, detailed chemical mechanistic information is still lacking.

#### A. Selective Reduction Studies

Four types of studies have been made, and these are: kinetic studies of reactions between O<sub>2</sub>/NO/NH<sub>3</sub> for temperatures near 1250K, kinetic studies of the selective reduction in post combustion environments, modelling studies, and demonstration studies. A brief description of each of these and their major finding is given to provide the reader with an overview of Thermal DeNO<sub>x</sub>.

Lyon<sup>3</sup> investigated NH<sub>3</sub>-NO-O<sub>2</sub> reactions in a quartz flow reactor at 1250K and found nearly quantitative reduction of NO in 75 msec. The products of reaction were not measured directly and were inferred since it was determined that the nitrogen containing products were not oxidizable to NO over a platinum catalyst at 1270K. Lyon states that this evidence eliminates all candidates except N<sub>2</sub> and N<sub>2</sub>O. The compound N<sub>2</sub>O was eliminated from further consideration through spectroscopic measurements. The other major product besides N<sub>2</sub> which was consistent with atom balance considerations was postulated to be H<sub>2</sub>O.

In a more extensive investigation of reactions of the NH<sub>3</sub>/NO/O<sub>2</sub> system in a quartz flow reactor, Lyon and Benn<sup>4</sup> monitored reaction progress by measuring O<sub>2</sub>, NO and NH<sub>3</sub> concentrations at different residence times. This was done as a function of initial reactant

concentration and temperature. Ammonia oxidation was found to occur in competition with the selective reduction of NO such that the NO concentration tends to approach a steady state value. A first order rate for NO decomposition was found to be consistent with the data over a temperature range of 1144 to 1226K. A reaction order of one half was determined for both  $\text{NH}_3$  and  $\text{O}_2$ . A free radical mechanism was discussed which gave a reasonable explanation of many of the features of the NO reduction.

In order to understand better the chemistry of  $\text{NH}_3$  oxidation which occurs in competition with the selective reduction of NO, Lyon et al.<sup>5</sup> investigated the oxidation at temperatures between 1250 and 1350K. In agreement with high temperature (2000K) shock tube results, ammonia oxidation is preceded by an induction time. No activation energy was given for the oxidation since the rate law describing  $\text{NH}_3$  disappearance changed functional form between 1310 and 1350K. The compounds  $\text{H}_2$  and NO were found to promote the  $\text{NH}_3$  oxidation rate, and  $\text{H}_2$  was also generated as a reaction product. Surface reactions on the quartz reactor walls were shown to be unimportant. The authors carefully reviewed reaction mechanisms previously useful in elucidating the features of high temperature  $\text{NH}_3$  oxidation, and argue convincingly that these mechanisms are inadequate for explaining their experimental results. Significantly more information is required on reactions of  $\text{NH}$ ,  $\text{NH}_2$ ,  $\text{HNO}$ , and other radical species to elucidate the kinetic mechanism of  $\text{NH}_3$  oxidation in the 1100 to 1400K temperature range.

Muzio et al.<sup>6</sup> studied the selective reduction of NO by  $\text{NH}_3$  in the post combustion environment of a laboratory scale combustion tunnel using natural gas as a fuel. The temperature at the injection point was varied over the range from 950 to 1860 K. Continuous gas analyzers

were used to measure  $O_2$ ,  $NO/NO_x$ ,  $CO$ , and  $SO_2$ , and standard electrodes were used to measure ammonia and cyano species. The reduction of  $NO$  was optimized at injector temperatures of 1230K and eighty percent  $NO$  reductions were achieved at a ratio of injected  $NH_3$  to initial  $NO$  of unity. In a later study, Muzio et al.<sup>7</sup> investigated the selective reduction in the post combustion environment of a firetube boiler modified to fire pulverized coal with preheated combustion air. Several types of coal with different sulfur content were used in this study. The optimum reduction temperature varied with coal type. Reduction of  $NO$  on the order of 55% could be achieved while limiting the  $NH_3$  breakthrough to less than 50 ppm with judicious selection of the temperature at the point of injection. The Muzio et al.<sup>6,7</sup> results and their relationship to our own will be discussed in detail subsequently.

Banna and Branch<sup>10</sup> investigated the selective reduction in the post combustion environment of lean premixed methane/oxygen/argon/ammonia flames. Secondary ammonia was introduced through injection holes distributed radially above the burner or through a secondary diffusion jet. Their experiment is unique since the product species  $N_2$  and  $H_2O$  were measured directly via gas chromatography. Their results indicate that  $NH_3$  oxidation is the dominant pathway at temperatures in excess of 1350K, and that optimum reduction of  $NO$  is achieved at 1220K. Both the oxidation and reduction were insignificant at temperatures less than 1100K. Reaction times on the order of .01 sec were reported.

In a combination experimental and modelling study, Lewis et al.<sup>11</sup> indicate that it also is possible to achieve  $NO$  reductions by injecting  $NH_3$  in a rich first stage in the 1600-1800K temperature range. Although specific analytical techniques are not mentioned, they report that neither

$\text{NH}_3$  nor HCN was detected in the product stream. Reductions on the order of 95% were achieved during their experiments. It is difficult to evaluate this study since many important experimental details are not given in the paper.

Modelling studies of the selective reduction have been performed by Saliman and Hanson<sup>8</sup> and Miller et al.<sup>9</sup> Each of these groups has performed isothermal plug flow calculations and attempted to characterize the selective reduction in the fully equilibrated post combustion environment of lean methane/air mixtures. Although each group uses a somewhat different set of reactions and kinetic parameters, each concludes that reactions between  $\text{NH}_2$  and NO are primarily responsible for NO removal and stress the significance of OH in influencing NO conversion. Each of these studies is plagued by insufficient kinetic data in the temperature range of interest.

The Thermal DeNO<sub>x</sub> process has been commercially demonstrated for gas and oil fired steam boilers and process furnaces. Two excellent reports<sup>12,13</sup> have been written under contract to the Environmental Protection Agency. One of these reviews the applicability of the Thermal DeNO<sub>x</sub> process to coal fired boilers and attempts to answer whether successful application of the process is related to boiler type. A cost analysis is performed on retrofit and new applications. The second report provides a technical assessment of the DeNO<sub>x</sub> process and places special emphasis on discussing the effects of temperature fluctuations and ammonia breakthrough in utility applications.

## II. DESCRIPTION OF THE EXPERIMENT

### A. Experimental Apparatus

The experimental apparatus used in this study consists of a laboratory scale combustion tunnel with associated control and measuring devices and the analytical instrumentation used to measure intermediate and product species concentrations. The combustion tunnel consists of a combustion section, an ammonia injection region, and a reaction and sampling section, and is illustrated in Figure 1.

Complete, stable, and reproducible burning of a fuel oil/air mixture is accomplished in the first section. All reactant flow rates are measured by rotameters calibrated with the appropriate fluid and are corrected for temperature and pressure variations. The tunnel pressure is near atmospheric, with only a slight vacuum ( $< 2$  torr) provided by the exhaust hood fans. Air is supplied by a laboratory compressor to a 5 cm inside diameter low alloy steel tube at the upstream end of the apparatus. Air flow rates can be varied from 3.3 to 35.0 gm/sec, but are nominally 9 g/sec. The fuel used throughout is #1 diesel oil, supplied by the Shell Oil Company. It has a measured density of 0.836 gm/ml. Elemental analysis of the oil yields a hydrogen/carbon ratio of 1.85, 0.04% by weight sulfur, and  $< 0.1\%$  by weight nitrogen. The fuel is delivered to a Monarch high pressure atomizing oil burner nozzle (Type R,  $30^\circ$  radius spray), and fuel flow can be set in the range from 15 to 42 gm/min, depending on the fuel pressure and nozzle size.

Two methods are used to achieve the NO levels typically found in the exhausts of commercial installations. Gaseous NO (Matheson CP grade) can be injected into the air supply upstream of the combustion section.

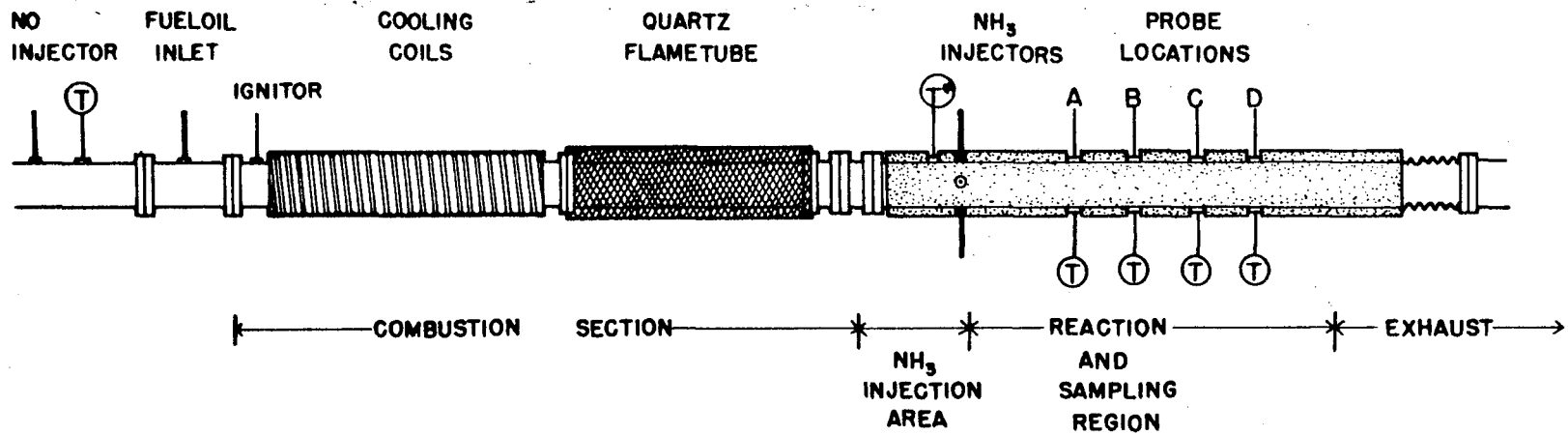


Figure 1. Schematic diagram of the laboratory scale combustion tunnel.

Another and somewhat more realistic method to simulate fuel-bound nitrogen compounds is accomplished by mixing pyridine (Mallinckrodt, research grade) with the fuel oil prior to addition to the fuel storage and delivery system. Fuel-bound sulfur compounds are likewise simulated by adding thiophene (Aldrich, gold label) to the fuel oil.

In order to simulate the Thermal Denox process in a utility, it is important to achieve stable, complete combustion of the fuel oil under a variety of conditions with the products thoroughly mixed prior to reaching the ammonia injection region. Rapid mixing and burning of the mixture is enhanced by several fixed disks located behind the fuel nozzle. Many different designs and placements were attempted in the early stages of the research, including the addition of several swirl blades before a successful arrangement was found. A 10 cm diameter section of steel tubing was installed immediately downstream of the fuel nozzle to increase the residence time of the reactants in the flame region. A quartz tube is located at the end of the combustion section which allows visual inspection of the flame, and aids in determining the sooting characteristics of the system. An acoustical vibration and feedback problem was mitigated by packing the air supply lines with steel wool and placing fixed and adjustable baffles in the exhaust line.

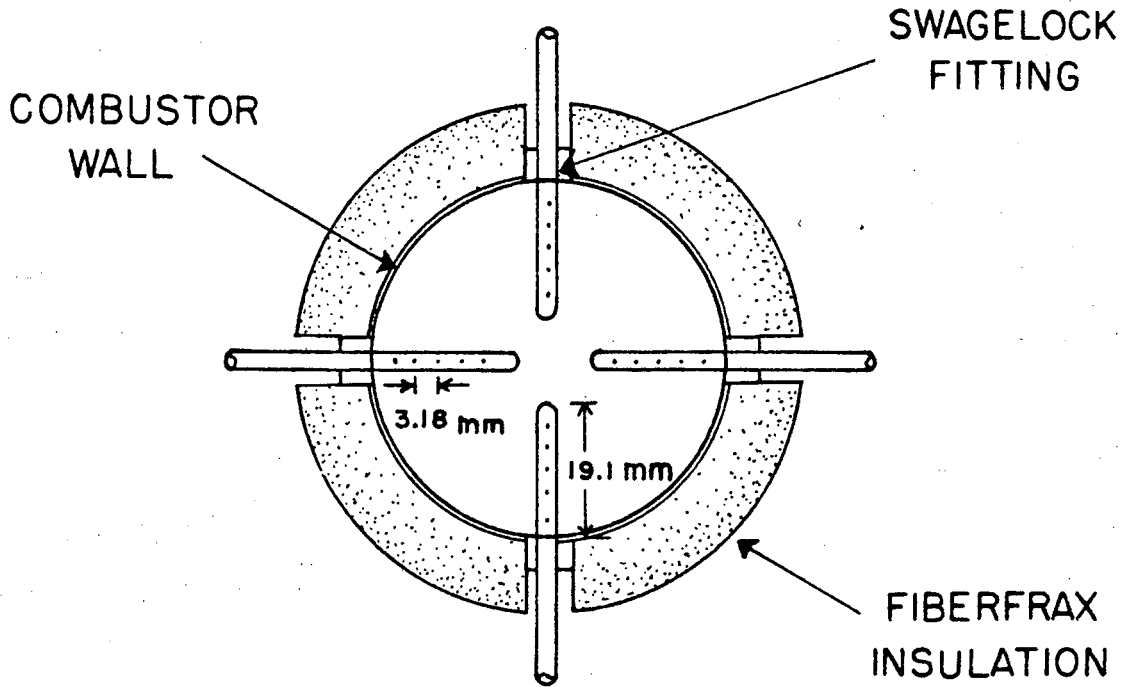
The temperature of the combustion products leaving the first section is adjusted by watercooling of the tunnel wall. Thirty meters of 0.6 cm copper tubing is wrapped around the 10 cm diameter section of the tunnel. Water flow rates up to 4 liters per minute through the tubing permits adjustment of the gas temperature to the desired values. The use of gaseous  $N_2$ , injected into the tunnel downstream of the flame, although used previously, was not used in this study since it resulted in cooling

which was too rapid to maintain equilibrium and changes in the overall mass flow rate.

Ammonia injection is accomplished by the system developed previously<sup>14</sup>. Mixtures of  $\text{NH}_3$  and  $\text{N}_2$  are introduced into the product gas stream through four symmetrically oriented quartz injectors, shown schematically in Figure 2. The injectors are positioned to supply the  $\text{NH}_3/\text{N}_2$  mixture counterflow to the combustion product stream, which aids in rapid mixing. Matheson CP grade anhydrous ammonia is used without further purification, and is mixed prior to being introduced into the injectors with gaseous nitrogen obtained from a 160 l liquid  $\text{N}_2$  tank which is passed through a heat exchanger to warm the gas to room temperature. An excess of  $\text{N}_2$  is injected to reduce changes in mixing due to variations in the  $\text{NH}_3$  flow. Previous experiments showed that the ammonia/nitrogen mixture does not react when passed through the heated quartz injectors<sup>15</sup>.

The reaction and sampling region begins immediately downstream of the ammonia injectors, and is ~60 cm long. This section, and parts of the ammonia injection region and exhaust lines, are insulated with layers of 2.5 cm thick Fiberfrax alumina silica insulation to reduce heat losses. Temperature or composition sampling can be performed at four different axial locations, separated by 12 cm. Each probe position has four tapped ports  $90^\circ$  apart to permit sampling in either the horizontal or vertical plane. Probes can also be positioned at a desired radial location by inserting machined stops in the port opposite the probe. The error in the radial probe position using this method is estimated to be  $\pm 1$  mm; however, this method requires cooling of the tunnel before a probe can be repositioned. Positioning of the probes while the combustor is continuously operating can be accomplished using marked probes. This method has the advantage of allowing many measurements to be taken under





### NH<sub>3</sub> QUARTZ INJECTORS

3.0 mm outside diameter

2.0 mm inside diameter

0.4 mm hole diameter

XBL 812-8267

Figure 2. Schematic diagram of the NH<sub>3</sub> injectors.

identical firing conditions with only a slightly larger error ( $\pm 2$  mm) in the probe position. Probe materials and methods will be described in the appropriate analytical technique description. After exiting the reaction section, the combustion gases are drawn into the main laboratory system exhaust.

## B. Analytical Techniques

### 1. Temperature Measurement

Temperatures are measured with bare wire Chromel/Alumel thermocouples. Corrections for radiation loss are made using measurements obtained from a suction pyrometer (aspirated thermocouple) using the same Chromel/Alumel junction. Figure 3 shows the correction as a function of temperature. The radiation corrections varied from 10K at a measured temperature of 1137K to 50K at a measured temperature of 1278K. All temperatures reported here are corrected by adding the appropriate radiation correction to the respective bare wire measurement: the accuracy of the temperature measurements are estimated to be  $\pm 5$ K. Experiments were also conducted to assess thermocouple precision. Three different thermocouples, made from different wire samples, were mounted together in a high temperature oven. The output of all three devices were measured to be within 3K at an oven temperature of  $\sim 1100$ K.

### 2. Sample Extraction

Gas samples are withdrawn from the reaction section through microprobes located at the four axial test port positions. The probes are constructed from 3.0 mm O.D., 2.0 mm I.D. quartz tubing, and are approximately 10 cm long. The tips of the probes are drawn down to an orifice diameter of 0.3 to 0.5 mm. This design is typically described as an "aerodynamically quenched" probe; however, recent evidence suggests that the primary quenching mechanism in probes of this type is convective cooling and not

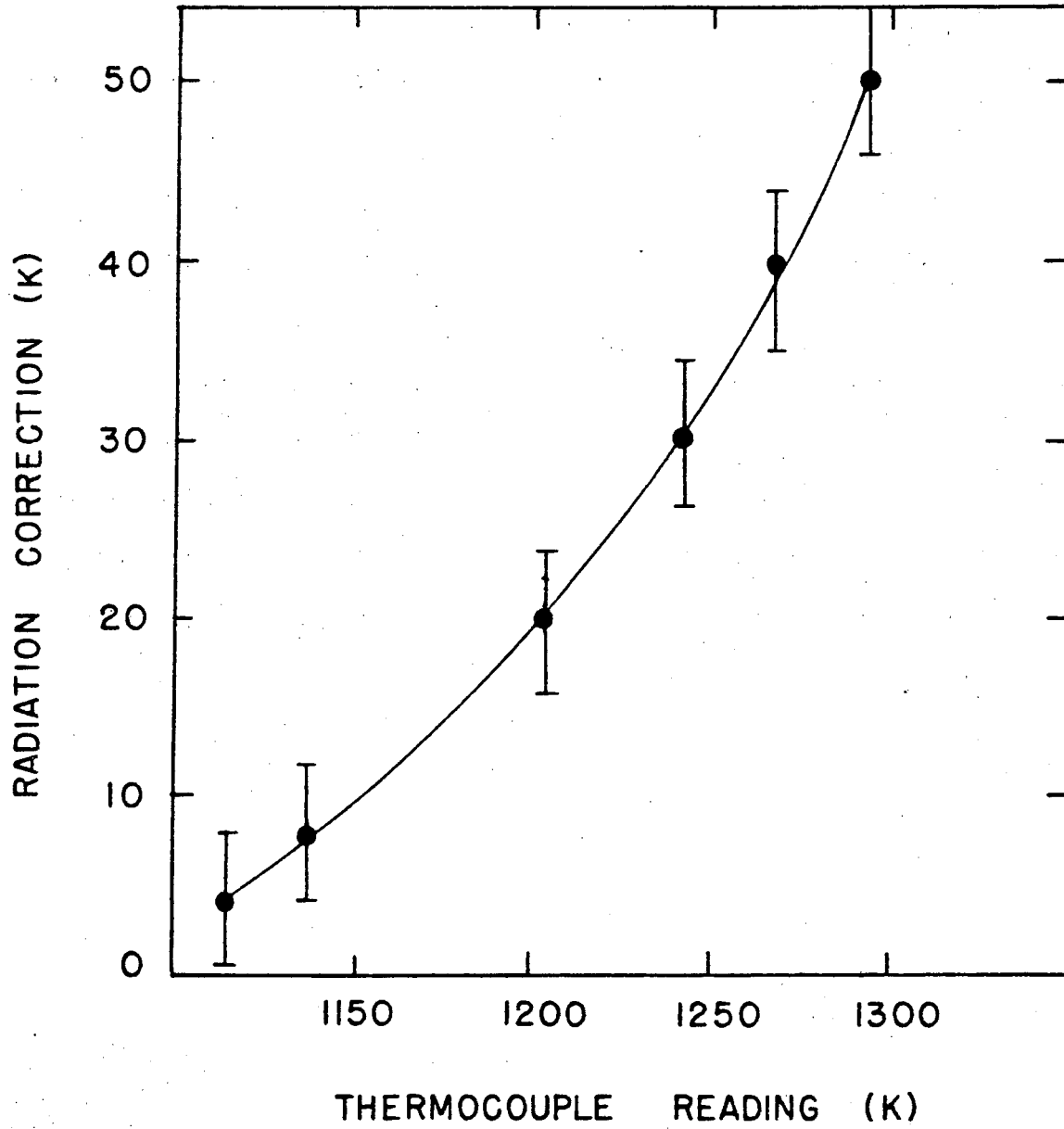


Figure 3. Radiation correction for Chromel-Alumel thermocouple determined by suction pyrometry.

aerodynamic quenching<sup>16</sup>. The sampling lines, pumping methods, and sample conditioning used depends on the specific method of analysis employed, and will be described with the appropriate analysis description.

### C. Species Analysis

#### 1. CO and CO<sub>2</sub> Measurements

Concentrations of CO and CO<sub>2</sub> are measured using Beckman Model 315 non-dispersive infrared continuous gas analyzers (NDIR). Metal bellows vacuum pumps, located in the analyzer housings, are used to withdraw the samples. Unheated Teflon lines are used to transport the gases to the analyzers. Water is removed through the use of two ice-bath cooled condensers in series. Calibration gases were obtained from different commercial vendors. Self-consistency of the gases and instrument linearity were checked by using several different calibration gas concentrations. Each instrument is calibrated immediately before and after measurements are taken. Several measurements were made without the use of the cold traps to determine if water condensation significantly altered the measured concentrations. Within experimental error (estimated to be 2%), no difference could be determined.

#### 2. H<sub>2</sub>O Measurements

Water concentrations are determined by inserting a pre-weighed magnesium perchlorate drying tube between the probe and a metal bellows vacuum pump. Heated Teflon lines are used to connect the probe to the drying tube. After exiting the pump, the volume of the now dry gas is measured with a calibrated wet test meter corrected for temperature, pressure, and water vapor concentration. The drying tube is weighed

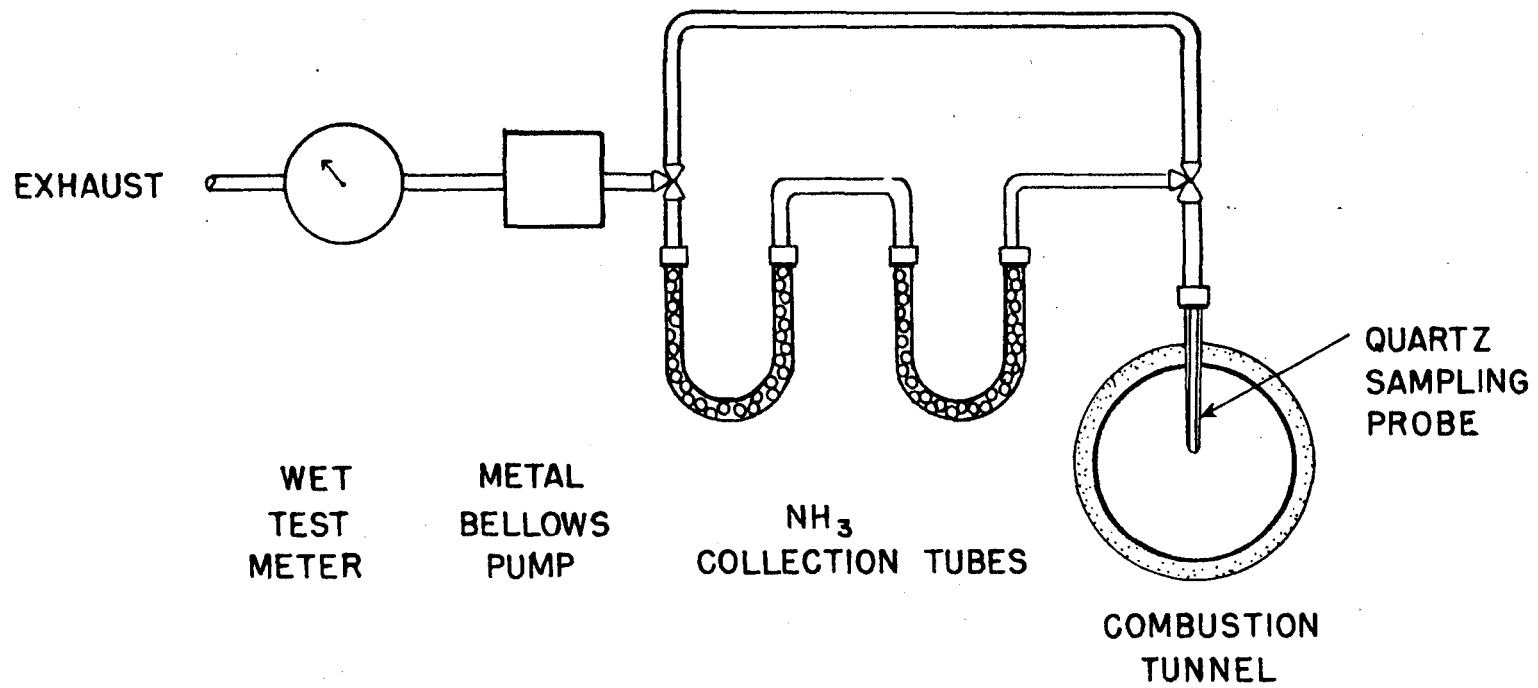
immediately after the exhaust is passed through it. The relative error in the accuracy of this method is estimated to be  $\pm 3\%$ .

### 3. NH<sub>3</sub> Measurements

In our previous report the precision and accuracy of the ammonia measurements were unsatisfactory. The problems have been corrected and we now have three reliable methods which will be briefly described.

A wet chemical method for ammonia analysis, based on the sodium phenolate method, has been developed in our laboratory. A sampling probe is connected by unheated Teflon lines to two pyrex U-tubes in series. The tubes are filled with 3 mm diameter pyrex spheres coated with a dilute ( $5 \times 10^{-3} M$ ) solution of phosphoric acid. A schematic of the collection system is shown in Figure 4. The sample gases are pulled through the tubes at a rate of  $\sim 100$  ml/min by a metal bellows pump which exhausts into a bubble flowmeter or a calibrated wet test meter. Two tubes are used in series to insure complete trapping of the ammonia.

Immediately after collection, the beads are transferred to 100 ml graduated cylinders. The tubes and adapters are rinsed several times with NH<sub>3</sub> free distilled water, with all of the washings added to the sample. Additional water is added to dilute the sample to a convenient volume. The dissolved ammonia is chlorinated to chloramine, NH<sub>2</sub>Cl, which is then reacted with sodium phenolate to form an indophenol dye of unknown structure with an absorption maximum at 632 nm. The optical density of the sample is measured against a blank in a Beckman DU spectrophotometer. For a 1.0 liter gas sample and a liquid volume of 60 ml, concentrations from 35 to 315 ppm can be measured. Different sample sizes can be used to extend the measurable concentration range.



XBL 812-8276

Figure 4. Schematic diagram of the ammonia collection system for the sodium phenolate method.

Possible interference by higher amines was examined by preparing known standards containing other amines. Ethyl amine exhibits an extinction coefficient of about 1/4 of that of ammonia. Dimethyl and higher amines show no interference. Other combustion exhaust products, with the exception of  $\text{SO}_2$ , do not alter the measurements. Absolute errors using this method are determined by measuring  $\text{NH}_3$  concentrations under cold flow conditions, and are estimated to be less than 10% when sampling combustion products. The method yields excellent results, but suffers from a low sampling rate and long analysis time. This technique is highly advantageous since it can be used as a reliable standard to determine if other methods yield consistent results.

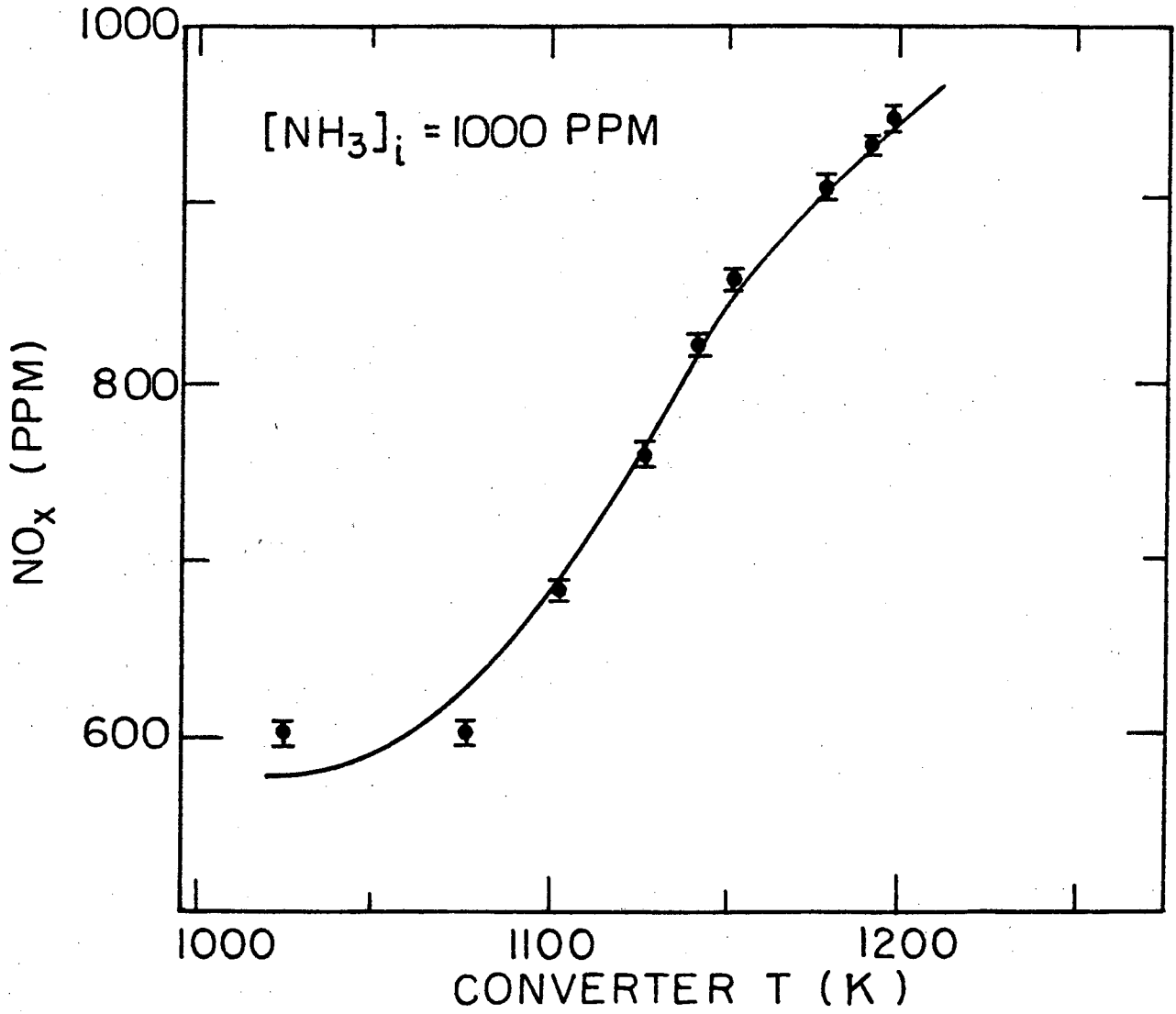
Perhaps the most convenient method for measuring  $\text{NH}_3$  is to oxidize it to NO on catalytic surface, followed by NO detection in a chemiluminescent analyzer. However, most NO analyzers are not equipped to handle the high concentrations of water vapor present in combustion exhausts. Condensation of water anywhere in the system can lead to large errors due to the high solubility of  $\text{NH}_3$  in water. In addition,  $\text{NH}_3$  is often adsorbed on many types of surfaces, especially metals. To avoid these problems, a ThermoElectron Model 12A chemiluminescent analyzer (CLA) was modified to prevent condensation and reduce the length of the sampling system that operates at near-atmospheric pressures. The capillary metering system has been mounted outside of the analyzer in a heated box, and is connected to the sampling probe by a 15 cm heated Teflon line. Reduced pressure (~30 torr) Teflon lines connect the capillary box to the stainless steel converter and reaction chamber in the analyzer housing.

The efficiency of the converter was measured using  $\text{NH}_3$ /air mixtures metered through calibrated rotameters. Converter efficiency as a function

of indicated converter temperature is shown in Figure 5. The converter is run at an indicated temperature of ~ 1200 K, the highest practical temperature that can be obtained. Converter efficiency as a function of  $\text{NH}_3$  concentration at this temperature is shown in Figure 6. All  $\text{NH}_3$  values reported that are measured by this method have been corrected for the converter efficiency.

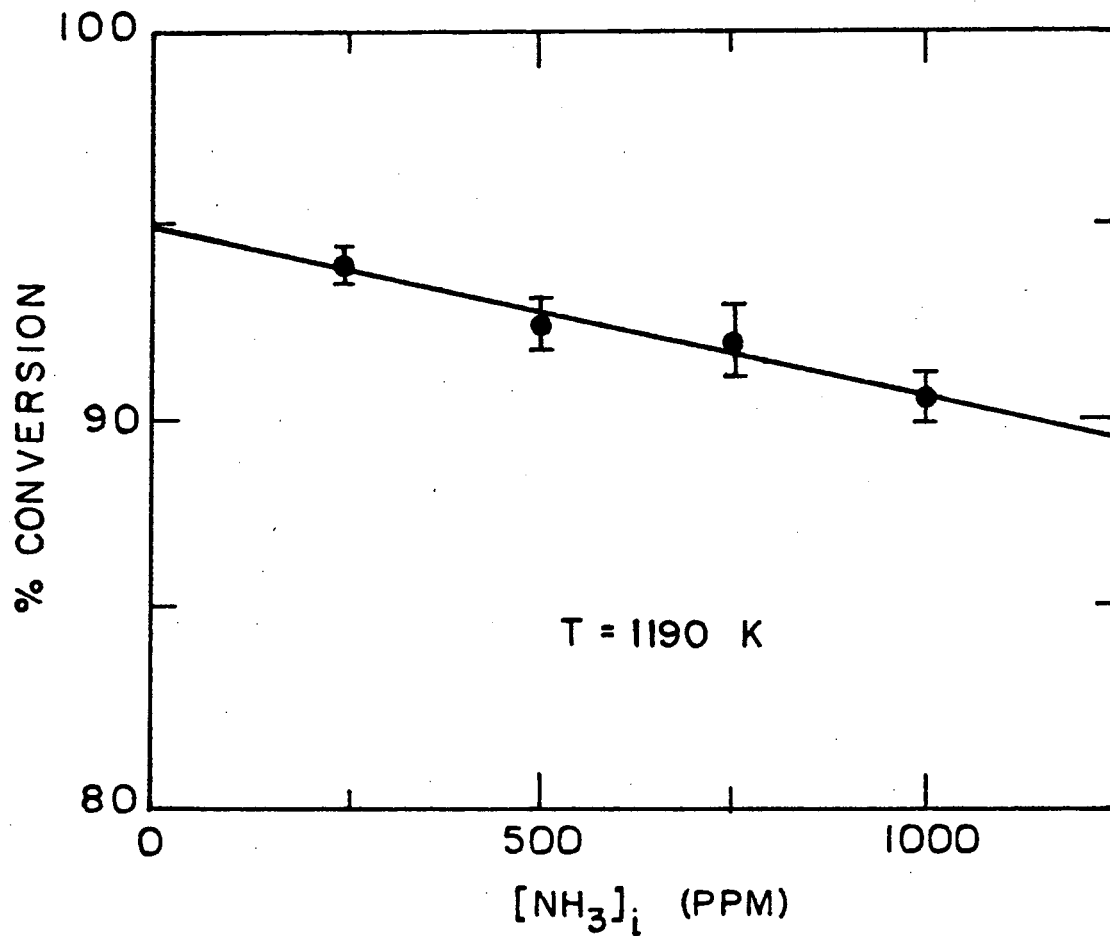
One of the major problems with the ammonia/chemiluminescent measurements is interference from other nitrogenous species, such as  $\text{NO}_2$ , that can be converted to  $\text{NO}$  under the same conditions<sup>17</sup>. It is thus necessary to use the phenolate method, which gives an independent measure of  $\text{NH}_3$ , to determine if the CLA method is free from interfering species. Table I lists the ammonia measurements made under cold flow conditions, where the  $\text{NH}_3$  values calculated from flow measurements are expected to be reasonably accurate. The phenolate method has been shown previously to give accurate results<sup>18</sup>. Table II lists the measured  $\text{NH}_3$  values using both methods under a variety of combustion conditions. In all cases, agreement is within experimental error of the methods. It should be noted that little or no reaction of  $\text{NH}_3$  and  $\text{NO}$  occurs in the catalytic converter of the chemiluminescent analyzer, even though the temperature of the converter is in the range employed in the Thermal  $\text{DeNO}_x$  process. This is probably due to the low pressure in the converter (< 20 torr), which reduces the number of collisions both in the gas phase and with the walls of the converter. At low fuel sulfur concentrations (<0.04%), no poisoning of the catalyst was observed. At fuel sulfur concentrations exceeding 0.4%, however, significant interference was observed. At these sulfur concentrations, ammonia measurements cannot be made with the chemiluminescent technique because





XBL 8012-13386

Figure 5. Conversion of NH<sub>3</sub> to NO as a function of converter temperature at a constant NH<sub>3</sub> concentration of 1000 ppm.



XBL 8012-13383

Figure 6. Conversion of NH<sub>3</sub> to NO as a function of NH<sub>3</sub> concentration at a constant converter temperature of 1190K.

TABLE I

COLD FLOW NH<sub>3</sub> MEASUREMENTS

[NH<sub>3</sub>] (ppm)

---

NO <sub>x</sub> METHOD <sup>a</sup>	CALCULATED <sup>b</sup>	PHENOLATE METHOD <sup>c</sup>
400	403	
547	536	
810	807	788
1079	1072	
1354	1382	

a) determined with chemiluminescent analyzer

b) determined from flow measurement

c) wet chemical phenolate method

TABLE II  
NH<sub>3</sub> MEASUREMENTS

<u>T* (K)</u>	<u>φ</u>	<u>[NO]</u> (ppm)	<u>[NH<sub>3</sub>] (ppm)</u>	
			<u>a</u> <u>NO<sub>x</sub></u>	<u>b</u> <u>PHENOLATE</u>
1100	.83	320	677	653
1169	.95	117	318	352
1229	.78	29	340	362
1233	.74	265	27	32
		31	249	274
1235	.73	350	8	12
		49	2	1
300	0	0	810	788

a) measured by chemiluminescent method

b) measured by the sodium phenolate method

of ammonia-sulfur reactions which form solids that condense in the sampling lines. The phenolate method, when used carefully, can still measure ammonia reproducibly under these conditions.

Ammonia can also be measured with a gas-permeable specific ion electrode (Orion Model 95-10). This technique is often used for ammonia measurements, with the ammonia collected by bubbling exhaust gases through a dilute acid solution. The  $\text{NH}_3$  can be collected quantitatively, but the  $\text{CO}_2$  that dissolves in the solution can lead to a 20% error in the electrode potential. This is due to two factors: the  $\text{CO}_2$ , hydrolyzed to a weak acid, alters the pH of the solution, and the change in the ionic strength (i.e. total number of dissolved species) can affect the solubility of ammonia. While this interference may be well known to electrochemists, it is not to many combustion researchers. It was found that the collection technique developed for the sodium phenolate method also works well for the ion analysis since small liquid volumes are involved in the collection procedures. When the  $\text{CO}_2$  interference taken into account, the ion electrode works as well as the sodium phenolate method. This method has the disadvantage of suffering from a large amine interference and is also plagued by low sampling rates and long analysis times.

#### 4. NO Measurements

The ThermoElectron Model 12A chemiluminescent analyzer, described in the  $\text{NH}_3$  measurement section, is also used to measure NO concentrations. Calibration gases of NO in  $\text{N}_2$  were purchased from commercial sources. Aluminum cylinders were specified for the gases, since previous experience indicated that NO can react when stored in iron tanks. Concentrations of the calibration gases were checked by mass spectrometer analysis and by

comparison with NBS standards. Instrument linearity was checked by dilution of NO samples with measured amounts of nitrogen.

The quenching of excited-state NO by H<sub>2</sub>O, CO<sub>2</sub>, and O<sub>2</sub> in an analyzer reaction chamber is being measured by another researcher in our laboratory<sup>19</sup>. Preliminary results indicate that analyzers with different reaction chamber geometries will have different quenching corrections. No measurements of quenching have been made on the type analyzer used in this study: thus, no meaningful correction can be made at the present time. However, extrapolation of the measured quenching rates yield an upper limit of ±5% for the absolute error in the NO measurements.

#### 5. HCN Measurements

Hydrogen cyanide was measured by a variety of techniques. The first, and the simplest, employed a Matheson Kitagawa detector tube kit. Samples are withdrawn through a probe into a Kitagawa tube that is connected to the probe by a short (~ 5 cm) piece of Teflon tubing. Alternatively, the probe is removed and the tube inserted into the hot gas stream that flows from the opening. The sensing limit claimed by the manufacturer is on the order of 0.2 ppm. The presence of more than 5 ppm SO<sub>2</sub> or 5 ppm NH<sub>3</sub> interferes with the HCN measurement, the former causing higher readings while the latter lowers the resulting measurement.

The second method employs an Orion Model 94-06 CN<sup>-</sup> ion electrode. Samples are collected using the glass bead method developed for the NH<sub>3</sub> measurements, with either a dilute acid or base used to coat the spheres. Using reasonable sized gas samples, a concentration of HCN in the gas phase of ~ 1 ppm should be measurable. The expected combustion products should not significantly interfere with the CN<sup>-</sup> measurement.

The third method, gas chromatography, is used to measure HCN and other nitriles. A Varian 3700 gas chromatograph is equipped with a flame ionization detector, and is interfaced to a Spectra-Physics IV B integrator. The column, 5% Carbowax 400 on Chromasorb T (TFE 6)<sup>20</sup>, has been successfully used to measure HCN at low ppm concentrations, and higher nitriles at unknown concentrations from combustion-type mixtures. Sample gases are pulled through a heated 5 cm<sup>3</sup> stainless steel sample loop by a rotary vacuum pump. The probe and sample loop are connected by a heated Teflon line approximately 1 meter in length. A calibration mixture of 106 ppm HCN in N<sub>2</sub> was prepared and stored in a stainless steel cylinder. The gas is periodically checked by mass spectrometer analysis to insure that the concentration of HCN is unchanged. The lower limit of detection for HCN is estimated to be in the 1 - 5 ppm range. Detection limits for other nitrogenous species have not been determined, but the flame ionization detector should be at least as sensitive for the other carbon-containing nitrogenous compounds as it is for HCN.

#### 6. Hydrocarbons, O<sub>2</sub> and N<sub>2</sub> Measurements

A Hewlett-Packard 5750 gas chromatograph with thermal conductivity and flame ionization detectors is used to measure a variety of compounds. The Spectra-Physics integrator is also used in this system. Two columns are used in an automatically switched configuration. One column is filled with Porapak Q, the other with MS-5A molecular sieve. Water is removed in an ice-cooled condenser before introduction into a 0.5 cm<sup>3</sup> sampling loop. A calibration mixture consisting of various hydrocarbons (CH<sub>4</sub>, C<sub>2</sub>H<sub>4</sub>, C<sub>2</sub>H<sub>6</sub>, C<sub>3</sub>H<sub>6</sub>, C<sub>3</sub>H<sub>8</sub>), CO and CO<sub>2</sub>, and N<sub>2</sub> is used. Hydrocarbons can be measured in the 0.01% range with reasonable accuracy. Air is also used to calibrate the instrument for O<sub>2</sub> and N<sub>2</sub>.

## 7. SO<sub>2</sub> Measurements

Sulfur dioxide is measured with a ThermoElectron Model 40 pulsed fluorescent analyzer. The instrument is equipped to remove water vapor present at concentrations below 2%, but since combustion product gases typically contain much higher water concentrations dilution of the sample gas is necessary. The product gases are withdrawn by a quartz sampling probe and are mixed with nitrogen gas in a heated Teflon manifold prior to analysis. Calibrated rotameters are used to measure the N<sub>2</sub> flow rate and the total exhaust flow rate from the analyzer, with the difference in the measured rates used to calculate a dilution factor. Quenching of excited SO<sub>2</sub> molecules by O<sub>2</sub>, H<sub>2</sub>O, and CO<sub>2</sub> is corrected for by assuming equilibrium concentrations of these species and using quenching coefficients obtained from the instrument manufacturer. Since the accuracy of the instrument is derived from the calibration gases, gas cylinders of different materials are being used to determine if SO<sub>2</sub>/N<sub>2</sub> mixtures are stable when stored for long periods. The absolute error in the SO<sub>2</sub> measurements, including the dilution factor, is estimated to be approximately 10%. It should be noted that SO<sub>2</sub> measurements cannot be made when NH<sub>3</sub> is present due to the formation and condensation of ammonia-sulfur compounds in the sampling system.

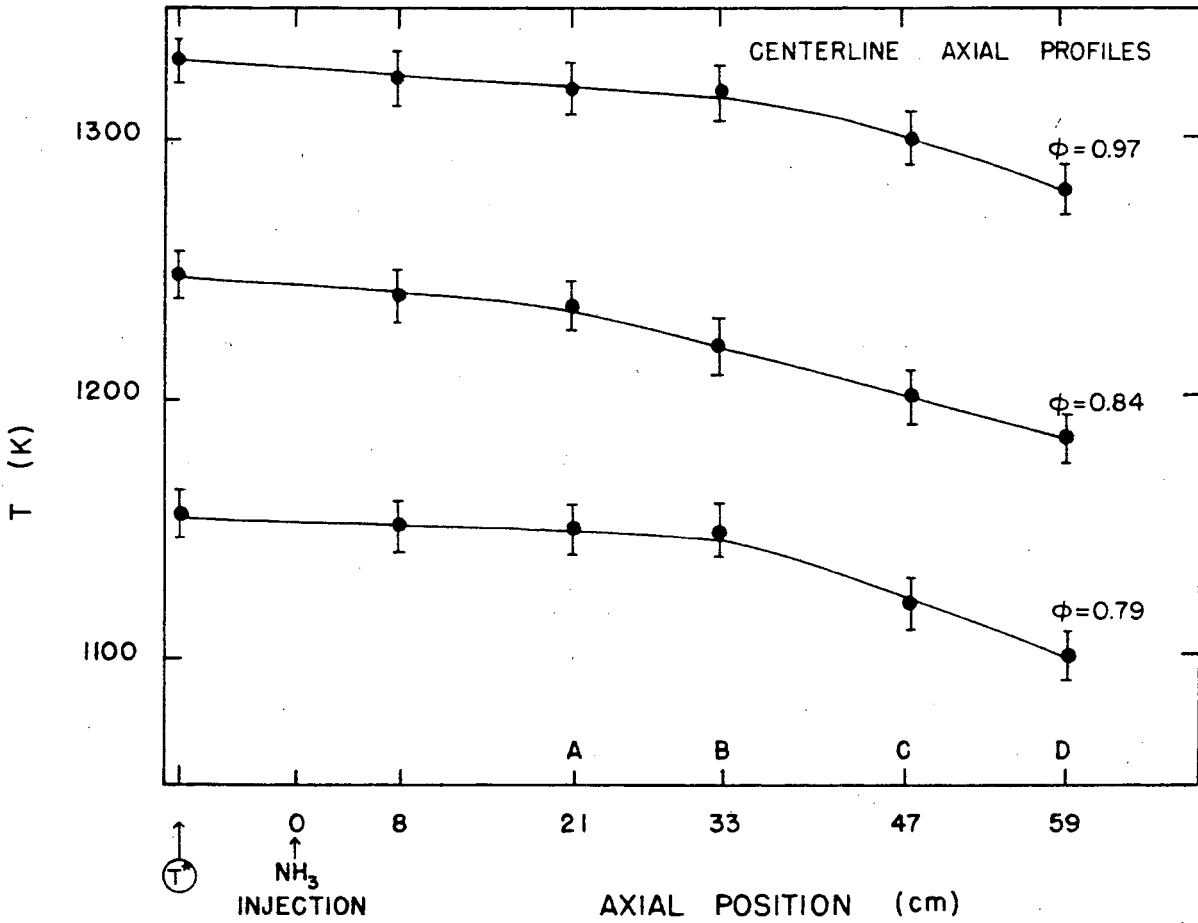


### III. SYSTEM CHARACTERIZATION

Prior to examining the reduction of NO by NH<sub>3</sub> addition, the performance of the combustion tunnel was characterized to obtain information on the uniformity and reproducibility of the experimental conditions. The combustion of the fuel oil spray, mixing of the post-combustion gases, and the injection and subsequent reaction of the NH<sub>3</sub> were quantified by measuring temperature and composition profiles in the apparatus in both axial and radial directions.

A significant and frequently mentioned parameter in the following paragraphs is the combustion product temperature at the point of ammonia injection. To avoid any confusion which might result from abbreviating this description to "NH<sub>3</sub> injection temperature" or "injection temperature", the combustion product temperature at the ammonia injection site will hereafter be referred to as T\* (Figure 1).

Axial and radial temperature profiles were measured in the reaction and sampling region for a variety of equivalence ratios and flow rates. A typical axial profile is shown in Figure 7. The axial gradients were found to be essentially linear with a slope of approximately 1 K/cm. Typical radial temperature profiles are shown in Figure 8, where the radial distance is measured from the combustor wall to the centerline of the tunnel. These profiles were measured at probe position B (see Figure 1). Radial profiles exhibit a shape characteristic of steady-state turbulent pipe flow which demonstrates the well mixed nature of the combustion products downstream of the ammonia injection site. The magnitude of the radial temperature gradient has only a weak dependence on the centerline temperature, but exhibits a much larger dependence on the total mass flow rate. At high throughputs the radial gradient is smaller, but the residence time of



XBL 812-8273

Figure 7. Combustion effluent temperature measured along the combustor test section centerline for three different equivalence ratios.

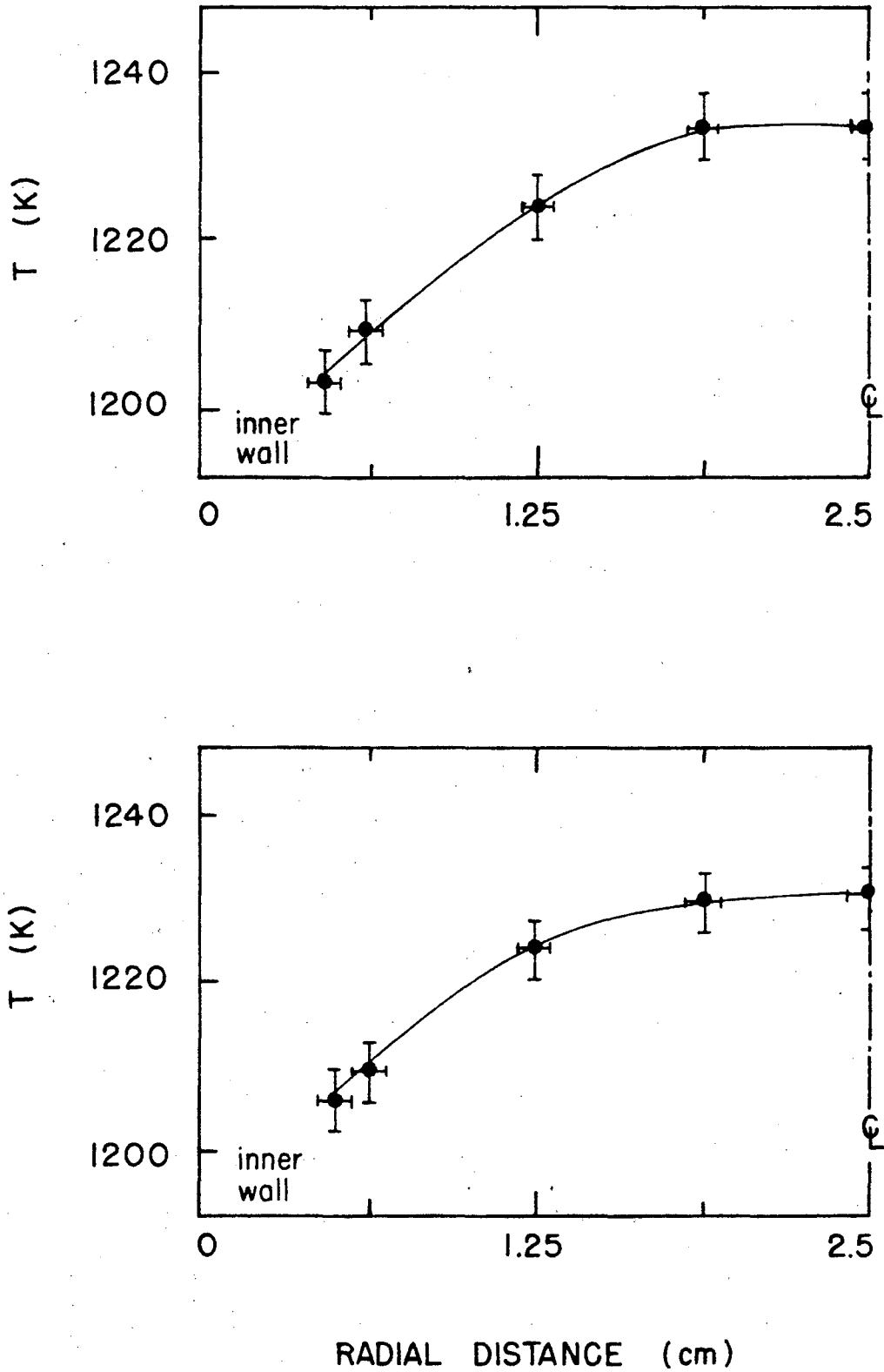


Figure 8. Combustion effluent temperature measured as a function of radial distance at probe position B, 33 cm downstream of the NH<sub>3</sub> injectors, for  $\phi = 0.89$  and flow velocities of a) 17 m/s and b) 21 m/s.

XBL 812-8272

molecules in the reaction section is reduced. An intermediate flow rate which results in an average velocity of about 17 m/s is used to yield reasonable radial gradients (20-25 K change from the centerline position to one ~ 80% of the distance to the combustor wall) while allowing approximately 40 msec reaction time.

Other indications of complete combustion are the absence of large temperature fluctuations, the uniform distribution of combustion products in the reaction section, and the agreement between measured concentrations calculated assuming equilibrium conditions.

When combustion of the fuel oil spray is obviously incomplete, the visible portion of the flame extends through the quartz flametube and into the reaction section, and is accompanied by anomalous thermocouple readings which exhibit large ( $\pm 50$  K) fluctuations. One thermocouple output is monitored continuously throughout each experiment to insure that no measurements are taken when this condition occurs.

Concentration profiles of CO and CO<sub>2</sub> were measured in both axial and radial directions. One set of CO<sub>2</sub> measurements is presented in Table III. The average concentration measured at  $T^* = 1236$  K and  $\phi = 0.68$  is 10.54%, within experimental error of the calculated equilibrium value of 10.43%. No significant axial or radial gradients were observed. Measurements of CO concentration profiles were consistent with the CO<sub>2</sub> results, again with no significant gradients present. At equivalence ratios less than 0.95, CO concentrations in the range of 40 to 60 ppm were measured. While these values are higher than the calculated equilibrium values, they are in good agreement with results obtained from similar combustion systems<sup>21</sup>. Measurements of O<sub>2</sub> and H<sub>2</sub>O were not as extensive as those for CO and CO<sub>2</sub>, but they were within experimental error of their expected equilibrium values.

TABLE III

CO<sub>2</sub> Concentration Profiles

<u>Probe Axial Position</u>	<u>Probe Radial Position†</u>	<u>[CO<sub>2</sub>] Dry, Volume %</u>
D	CL	10.52
C	CL	10.55
B	CL	10.52
D	CL - 1/2	10.49
D	CL	10.52
D	CL + 1/2	10.56
D	CL + 3/4	10.57
D	CL - 3/4	10.55

Average [CO<sub>2</sub>] = 10.54 ± .03%

T\* = 1236 K      φ = 0.68

† Radial probe position centerline is CL; fractions indicate fraction of distance from centerline to combustor wall.

No unburned hydrocarbons were ever detected when combustion occurred under lean conditions.

Nitric oxide levels were also measured before adding nitrogenous compounds to the fuel. This thermal NO concentration was found to be somewhat dependent on the equivalence ratio and  $T^*$  value. At a fixed temperature and equivalence ratio, however, no concentration gradients were observed in the reaction section. For lean mixtures and  $T^*$  values from 1100 to 1350 K, NO measurements were in the range of 35-65 ppm. These concentrations are reasonable for the conditions employed and show the expected dependence on equivalence ratio and temperature. Measurements made in the  $\text{NO}_x$  mode of the chemiluminescent analyzer prior to the addition of  $\text{NH}_3$  indicate that  $\text{NO}_2$  concentrations are less than 2 ppm, and this suggests that probe effects are not significant for these experimental conditions.

The equivalence ratio in this study varied from 0.6 to 0.95. Rich combustion was attempted but stable and reproducible burning of a fuel oil spray under rich conditions could not be achieved. Problems arise from two sources when the equivalence ratio exceeds 1.0: the visible flame length increases until it extends into the reaction and sampling region, and significant sooting occurs throughout the combustion region. This restriction is not severe, since practical combustion systems operate under lean-burning conditions.

#### A. $\text{NH}_3$ Mixing Conditions

The rapid and thorough mixing of the  $\text{NH}_3/\text{N}_2$  mixture with the combustion exhaust is crucial in the control of the selective reduction process. Mixing characteristics were determined by flowing  $\text{NO}/\text{N}_2$  mixtures through the  $\text{NH}_3$

injectors. It was previously determined that less than 4% of the NO reacted when passed through the flame zone of a lean flame<sup>14</sup>. It can thus be expected that any NO introduced through the NH<sub>3</sub> injectors will remain unreacted as it passes through the sampling region. After initial adjustment of the injector positions under cold flow conditions, final adjustments are made under combustion conditions. One set of these measurements is presented in Table IV. The measured NO concentrations fluctuated randomly around an average value with the range of these fluctuations reported in the last column of the table. Injectors were adjusted until all NO readings downstream of probe position A were within 10% of each other. This method is extremely sensitive to injector malfunctions or misalignment. The ease with which NO measurements can be made allows for routine checks on the mixing performance.

#### B. Reduction of NO by NH<sub>3</sub>

Our investigation of the selective reduction of NO by NH<sub>3</sub> addition will be discussed in three sections, divided according to the type of fuel nitrogen and sulfur admixed with the fuel oil or air. The first section describes NO reduction when NO itself is used as the prototype fuel nitrogen compound. The second examines the experiments where pyridine is used as the principal source of NO, and the third covers experiments with both pyridine and thiophene added to the fuel oil.

It is important to discuss the meaning of the term initial NO concentration since there is much confusion regarding this term in the literature. There are two NO sources in our experiments: one is the result of prototype fuel nitrogen compounds, and the other is the thermal NO formed during the combustion process. Two different prototype fuel nitrogen compounds, NO and pyridine, were used in this study. The term initial NO concentration,

TABLE IV

NH<sub>3</sub> Injection System Mixing Characteristics

<u>Probe Axial Position</u>	<u>Probe Radial Position</u>	<u>[NO] ppm†</u>
B	CL	600-620
	CL + 1/2	610-630
	CL - 1/2	620-640
	CL - 3/4	590-610
	CL + 3/4	620-650
C	CL	620-630
	CL + 1/2	600-610
	CL + 3/4	600-620
	CL - 1/2	590-610
	CL - 3/4	570-580
D	CL	600-620
	CL - 1/2	610-620
	CL + 3/8	600-610
	CL + 3/4	580-590
	CL + 1/2	590-610

† Range of values indicate concentrations measured over ~ 1 min. Fluctuations measured over the same time with calibration gases were ± 1 ppm.

Operating Conditions:  $\phi = 0.89$ ,  $T^* = 1220$  K



$[\text{NO}]_i$ , will be used here to designate the total NO concentration measured in the reaction section when no  $\text{NH}_3$  is added. This concentration can be monitored at the final probe station since measurements of NO concentrations exhibited no axial or radical gradients for the conditions studied.

The experiments were designed to determine the effects of changing experimental variables such as the equivalence ratio, the combustion product temperature ( $T^*$ ), the amount of  $\text{NH}_3$  added, and the amount of fuel nitrogen and sulfur. Product emissions were determined for the range of variables investigated. Particular emphasis was placed upon monitoring "odd nitrogen" compounds (nitrogenous species other than  $\text{N}_2$ , NO,  $\text{NO}_2$  and  $\text{NH}_3$ ). The equivalence ratios given in the following figures were calculated from the measured flows of the reactants. Because of the uncertainties associated with the rotameters, the error in the equivalence ratio is estimated to be  $\pm 5\%$ , or approximately  $\pm 0.05$ . The reproducibility in the metering system is much better, as evidenced by our ability to closely reproduce ( $\pm 5\text{K}$ ) a  $T^*$  value for a given set of flow conditions. The amount of  $\text{NH}_3$  added in these experiments is normalized to the initial NO concentration, and is defined as  $\beta = [\text{NH}_3]_i / [\text{NO}]_i$ . The uncertainty in a  $\beta$  value is estimated to be  $\pm 3\%$ . The concentration of fuel nitrogen or sulfur when pyridine or thiophene is used is calculated from the physical properties of the compounds which are added volumetrically to the fuel supply. The calculated values presented have an estimated error of  $\pm 5\%$ . Elemental analyses were also performed on selected samples to confirm the fuel composition<sup>22</sup>.

Experiments were performed with  $\text{NH}_3$  injection to insure that the residence time in the reaction section was sufficient to allow complete

reaction before the gases entered the exhaust line. Axial and radial NO and NH<sub>3</sub> concentrations were monitored in order to determine reaction progress. One set of centerline measurements, performed at  $\phi = 0.83$  and  $T^* = 1224\text{K}$ , is presented in Figures 9 and 10. For the range of conditions employed in this study, the reaction between NO and NH<sub>3</sub> is essentially complete (>95%) by the final probe station, with most (>85%) of the ultimate NO reduction occurring by probe position B 33 cm downstream of the NH<sub>3</sub> injectors. Ammonia concentration profiles corroborate these results. Measurements of this type allow us to present measurements only from probe position D with confidence that the reduction reaction is complete. These measurements also enhance the significance of the  $T^*$  temperature values presented, since the axial temperature gradient is small (~30K) in the region where most of the reaction takes place.

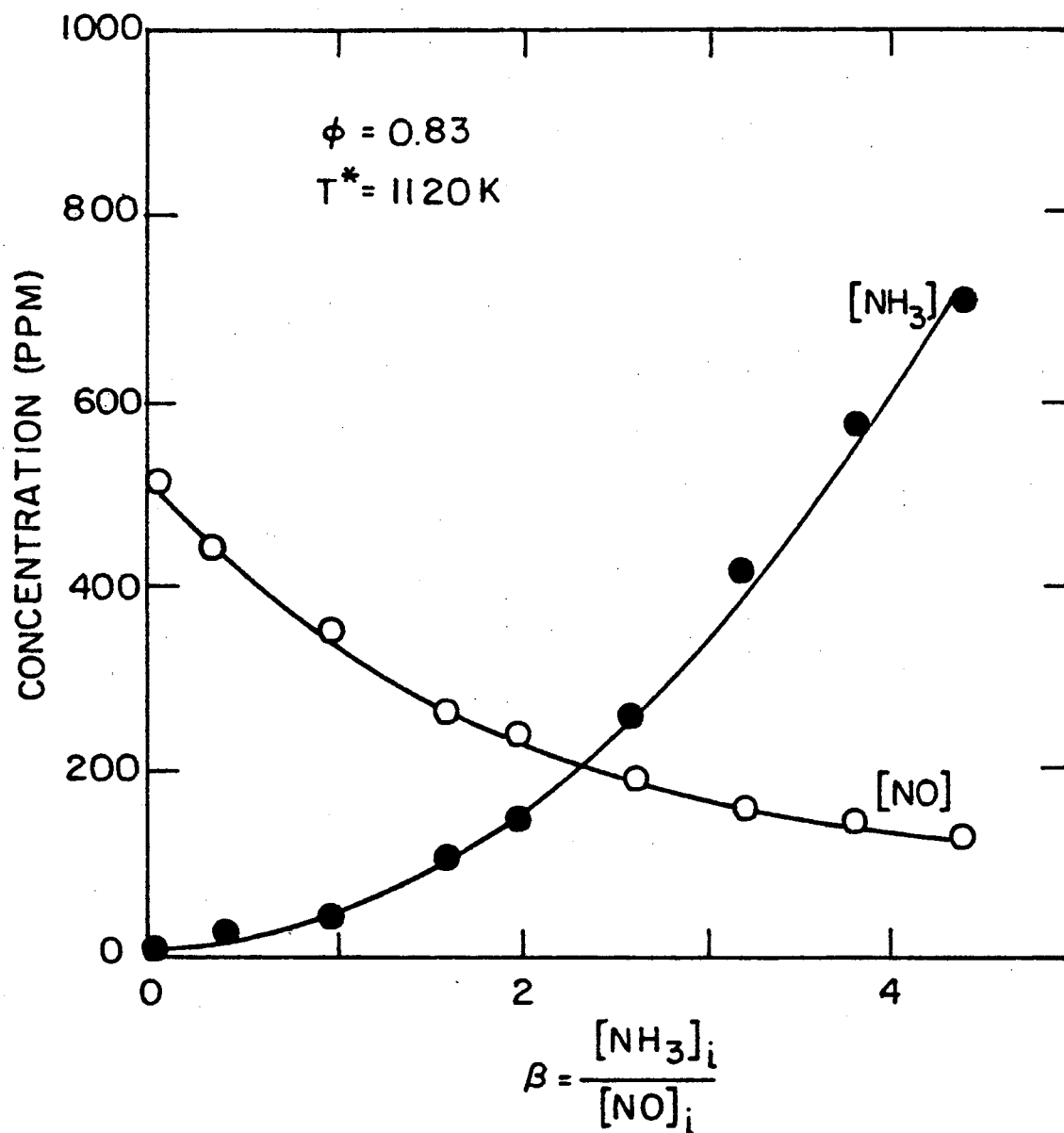
#### IV. RESULTS

##### A. Fuel Nitrogen: NO

The first set of experiments on the reduction process employed NO, injected into the air supply upstream of the fuel nozzle, as the prototype fuel nitrogen compound. The NO was metered until the initial NO concentration downstream,  $[NO]_i$ , was measured to be  $500 \pm 10$  ppm. The amount of NO decomposition through the combustion zone was determined by first setting the NO flow as described above, and then introducing the same flow of NO through the  $NH_3$  injectors while monitoring the NO level at the final probe station. The amount of NO that survived through the flame zone depended markedly on the equivalence ratio, with only small variations for different  $T^*$  values. Survival of NO ranged from ~78% at  $\phi = 0.95$  to ~95% at  $\phi = 0.83$ .

During these experiments much effort was directed toward achieving reproducible results and developing the analytical techniques necessary for the accurate measurement of product concentrations, especially those for nitrogenous species; thus not as many parametric measurements were made and the uncertainties in the optimum conditions for the reduction process are somewhat larger than those of subsequent experiments.

Figure 11 shows the results of the reduction of NO by  $NH_3$  at a fixed temperature ( $T^* = 1120K$ ) and equivalence ratio ( $\phi = 0.83$ ) as a function of  $\beta$ . The final NO concentration,  $[NO]_f$ , is defined as the measured value of NO at the centerline of the final probe station when  $NH_3$  is added to the combustion products. Two trends are observed which are common to all experiments involving NO or thiophene addition



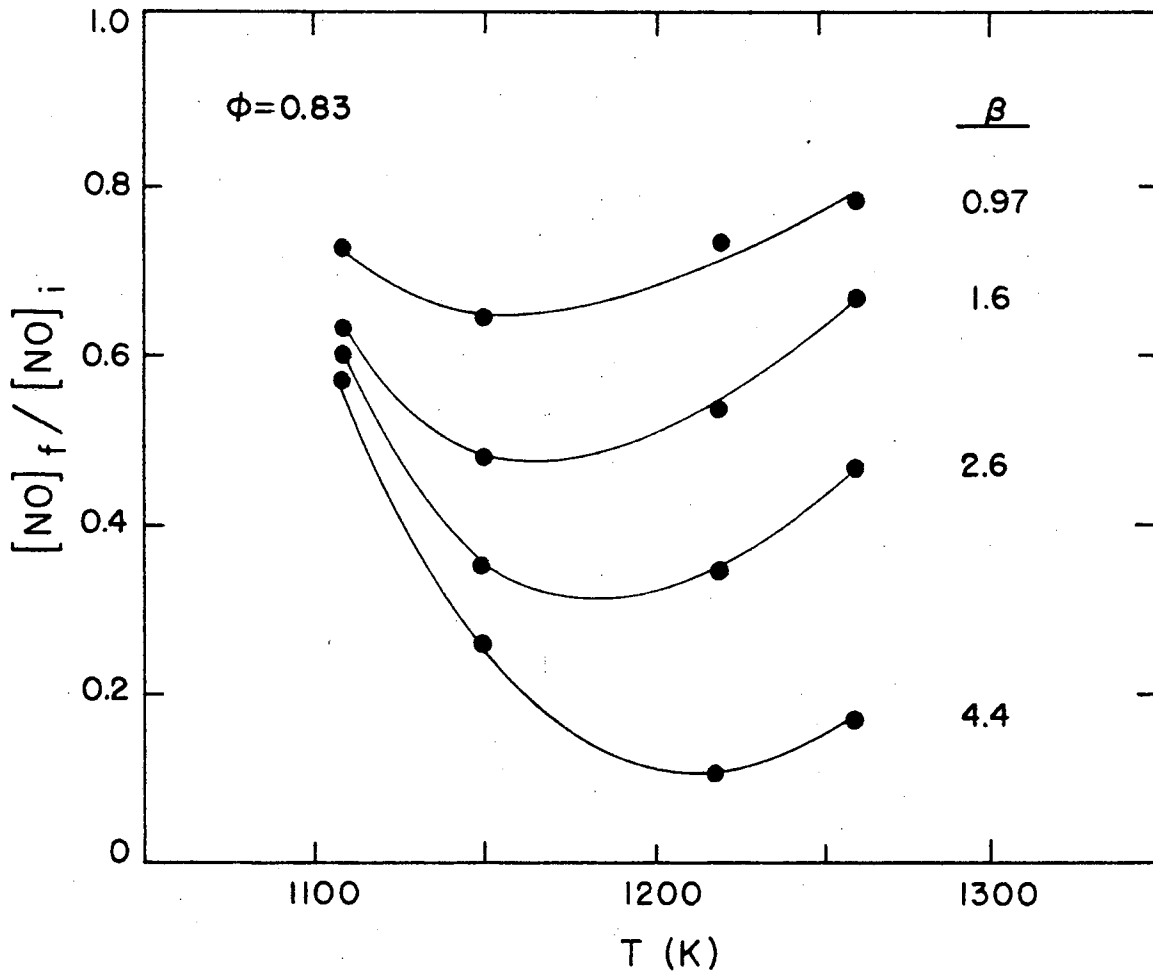
XBL 8012-13387

Figure 11. Concentration of NO and NH<sub>3</sub> measured centerline at probe position D as a function of  $\beta$  for  $\phi = 0.83$  and  $T^* = 1120K$ .

to the fuel supply: as more ammonia is injected, more NO reduction occurs, even at  $\beta$  values greater than 4.0; and the ammonia breakthrough increases with increasing  $\beta$ . The smooth character of the data points is an indication that the experimental conditions are well controlled and reproducible. This is especially relevant in the ammonia measurements, which previously were subject to large uncertainties and were not reproducible.

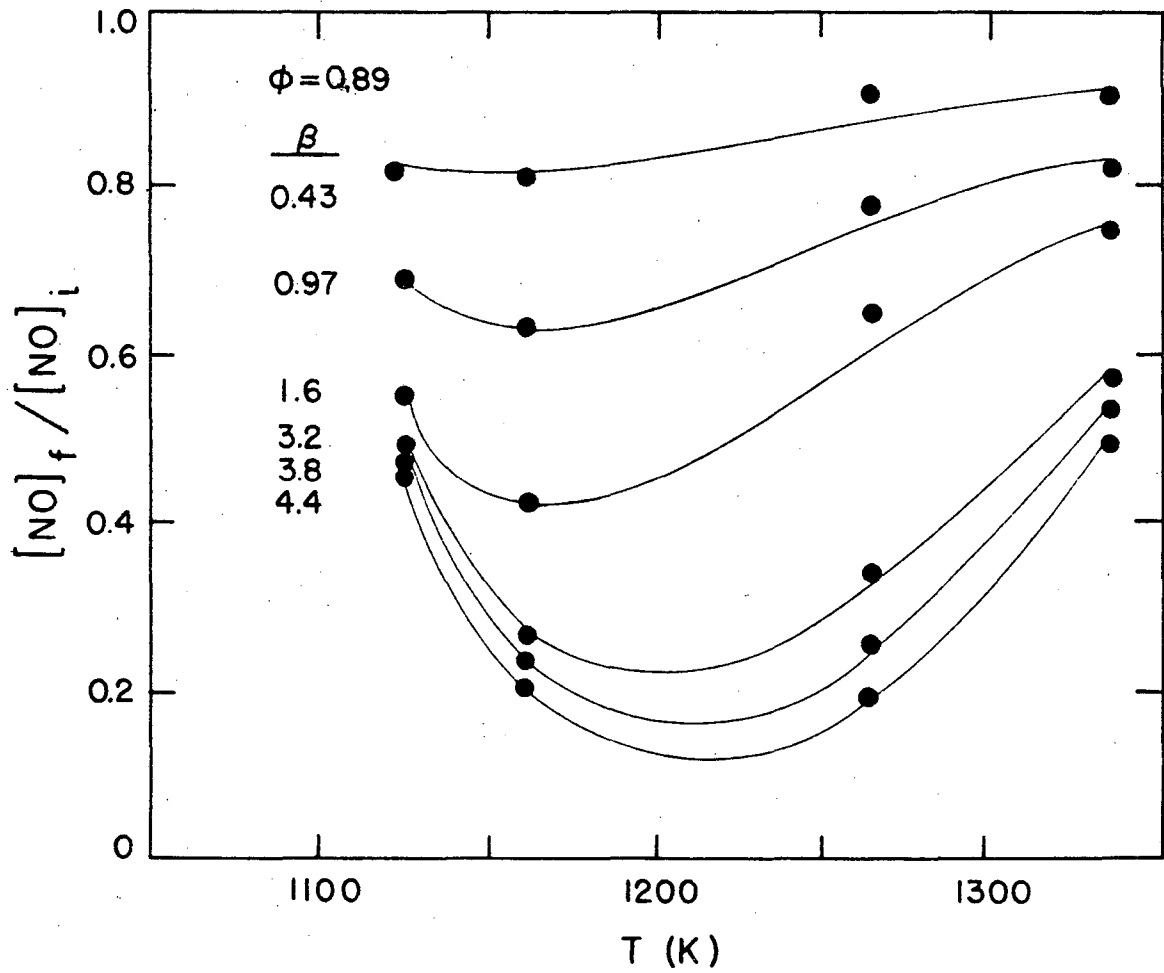
Determination of the temperature at which maximum NO reduction occurs at a fixed equivalence ratio is shown in Figures 12, 13, and 14. The reduction process shows a dependence on both the ammonia concentration and the equivalence ratio. At a fixed equivalence ratio, the optimum reduction temperature increases with increasing  $\beta$ . At high  $\phi$  values this trend is less obvious, and it becomes more apparent at leaner conditions. The range for the optimum reduction temperature varies from ~1150 to values in excess of 1250K. The fraction of NO reduced,  $[NO]_f/[NO]_i$ , depends on  $T^*$  and  $\beta$  but does not vary significantly with changes in  $\phi$ . For example, at  $\beta \approx 2.5$ , the maximum NO reductions, while occurring at different  $T^*$  values, is ~0.7 for all three equivalence ratios.

Ammonia breakthrough, the concentration of ammonia measured at the final probe station, is presented in Figure 15 for an equivalence ratio of 0.83. The results show that the temperature is the dominant factor in determining the concentration of ammonia remaining after the reduction process. The measured values were obtained using the chemiluminescent technique which were periodically compared with measurements made with the sodium phenolate techniques. For the range of conditions covered in Figure 15, the fraction of NO remaining after reduction ranges from ~0.1 to 0.8, corresponding to concentrations of



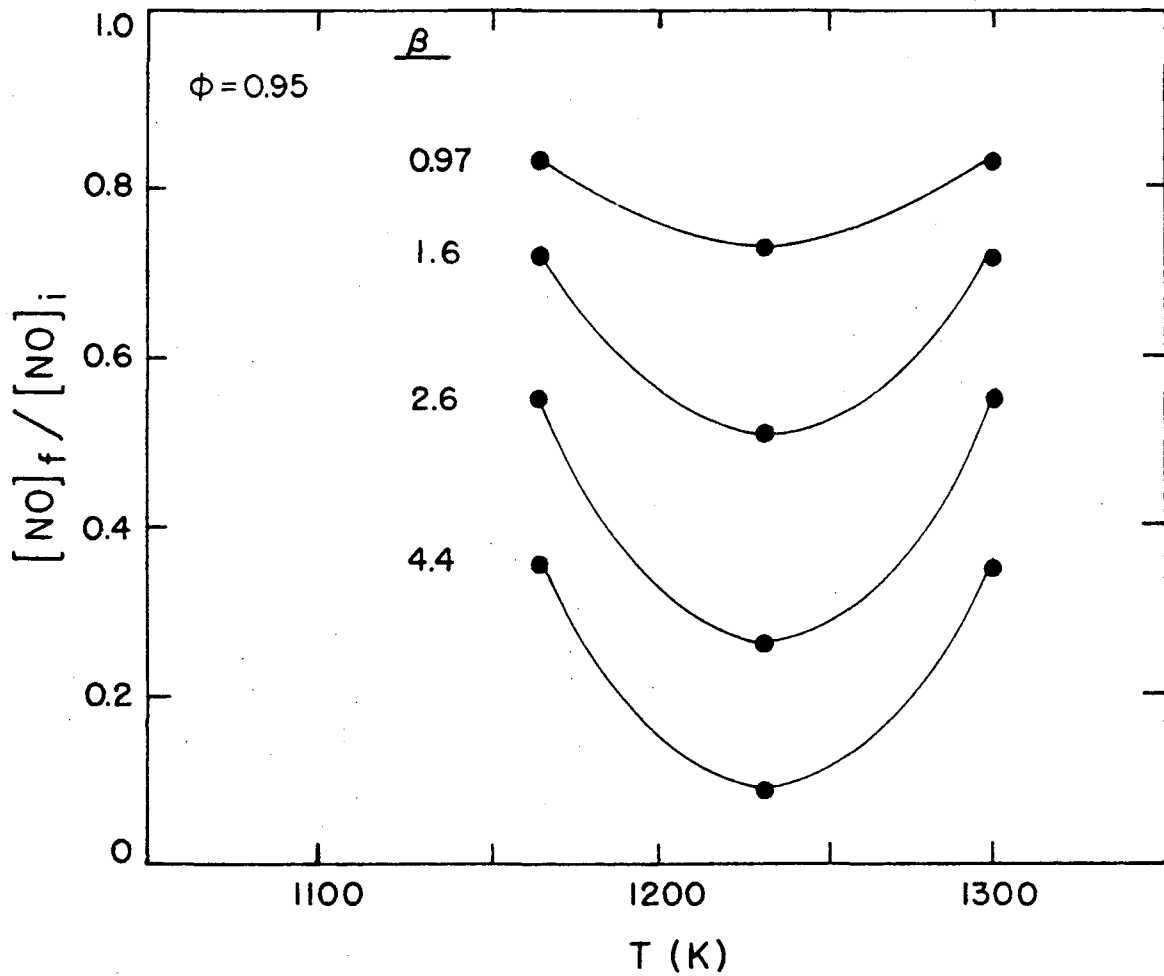
XBL 812-8269

Figure 12. The NO survival as a function of  $\beta$  and  $T^*$  for  $\phi = 0.83$  with NO as the fuel nitrogen.



XBL 812-8268

Figure 13. The NO survival as a function of  $\beta$  and  $T^*$  for  $\phi = 0.89$  with NO as the fuel nitrogen.



XBL 812-8270

Figure 14. The NO survival as a function of  $\beta$  and  $T^*$  for  $\phi = 0.95$  with NO as the fuel nitrogen.



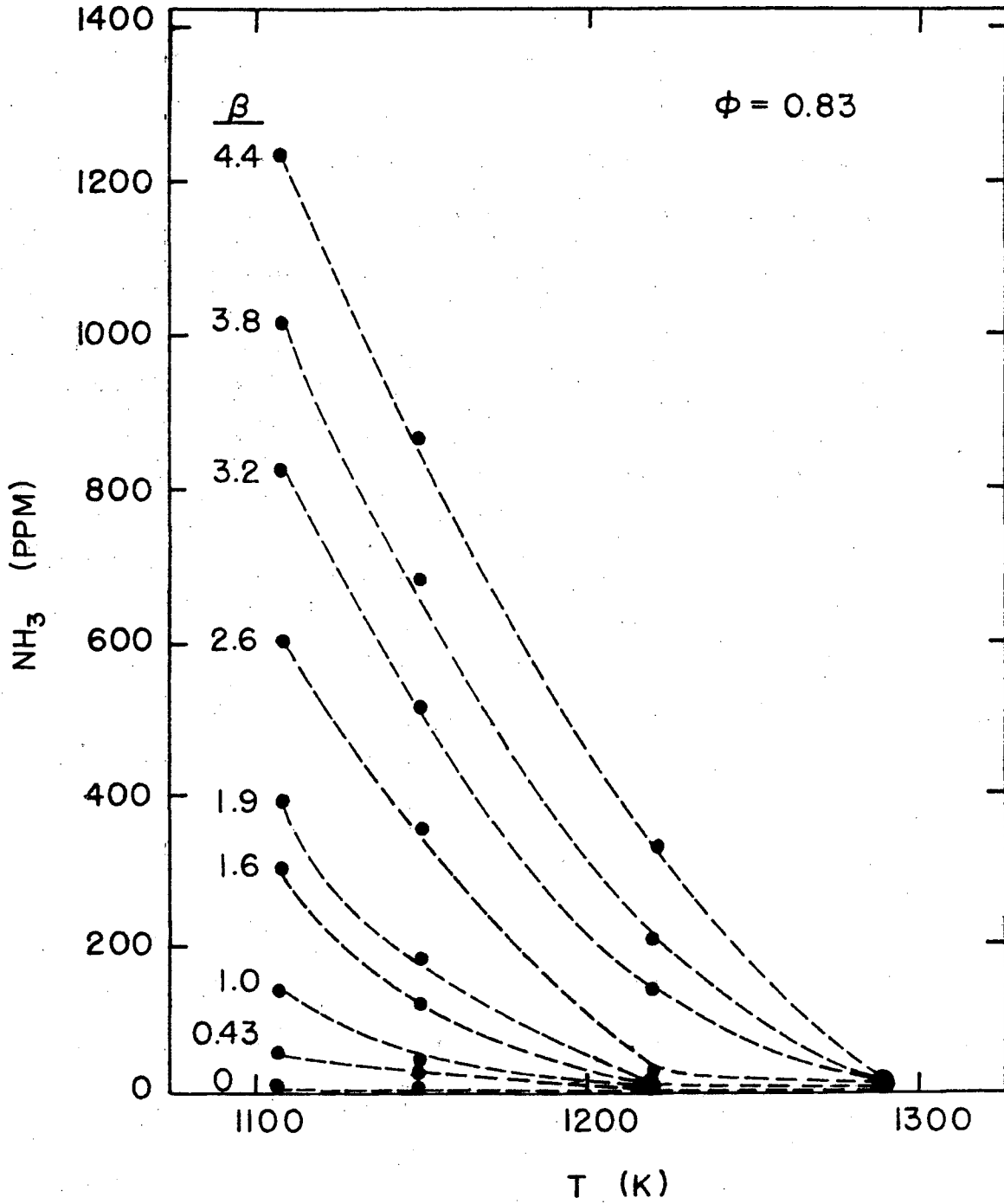
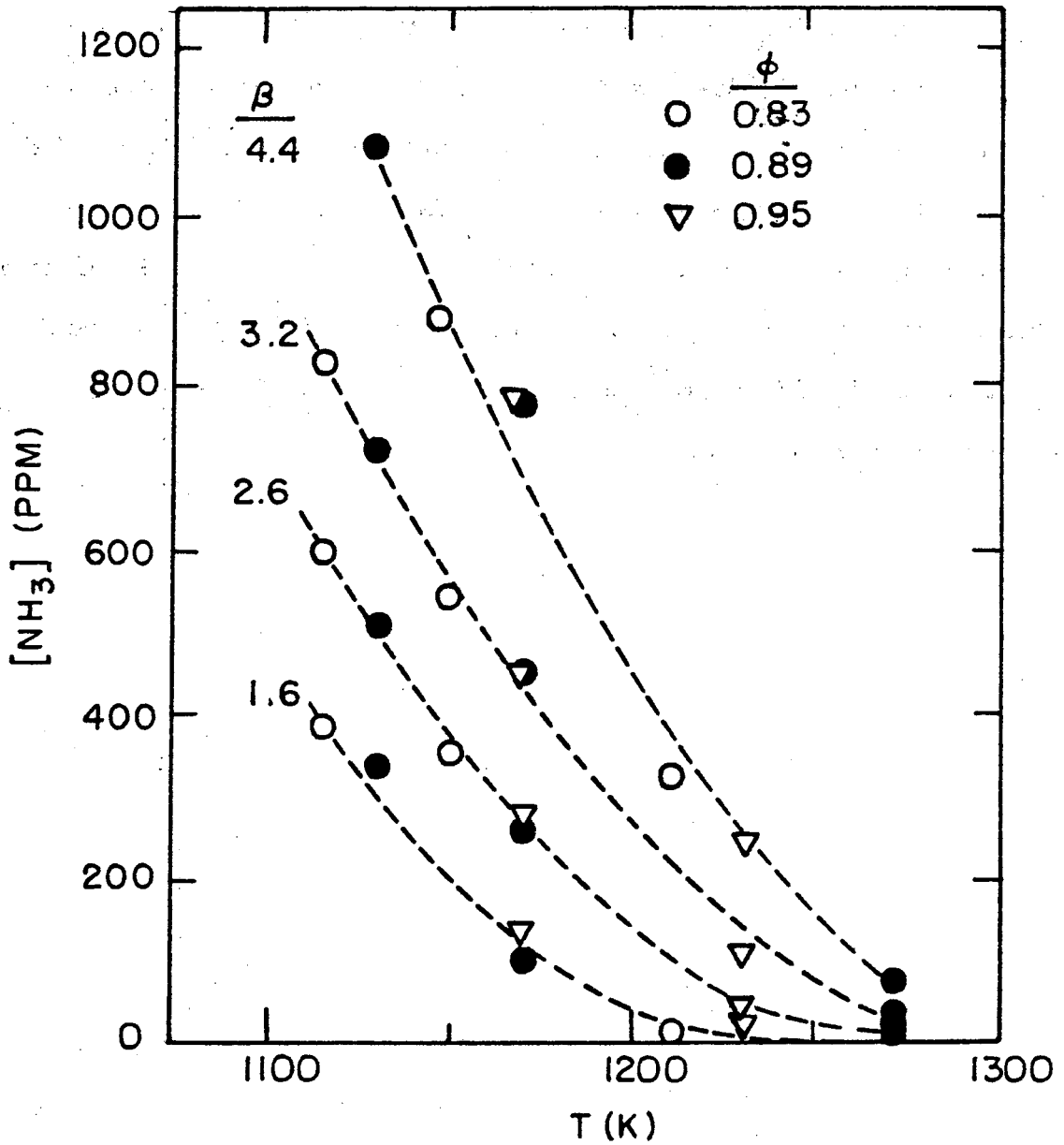


Figure 15. The  $NH_3$  breakthrough measured at probe position D as a function of  $\beta$  and  $T^*$  for  $\phi = 0.83$ .

50 to 400 ppm. The level of NO reduction appears to have no effect on the ammonia breakthrough, additional evidence that the reaction is complete by the final probe station. Figure 16 shows ammonia breakthrough for the three different equivalence ratios, measured by the CLA, sodium phenolate, and specific ion electrode methods. The agreement between the techniques is within the experimental error of the measurements, and is a strong indication that no interfering species (other nitrogenous compounds besides  $N_2$ , NO, and  $NH_3$ ) are present in any measurable quantities in this system. No significant differences in the ammonia concentrations were seen at the different equivalence ratios, suggesting that the oxygen concentration is not a limiting factor for the reduction reactions in lean combustion product gases.

Numerous attempts were made to measure HCN or other "odd nitrogen" species, employing all of the methods described in the experimental section. Concentrations of HCN were found to be below 1 ppm (the lowest detectable concentration) for all conditions studied, even when  $\beta$  values  $>4.0$  were used with temperature values that allowed for only slight reduction of NO concentrations. There was no evidence for any other "odd nitrogen" compound measurable on the gas chromatographic and gas chromatographic/mass spectrometric equipment. These results corroborate the ammonia measurements that show no measurable concentrations of interfering nitrogen compounds. It should be noted that no hydrocarbons or  $H_2$  were observed in the product gases during these experiments.

Because no measurable quantities of "odd nitrogen" species were observed for the conditions, experiments were undertaken to show that nitrogenous species could be measured at low concentrations when



XBL 8012-13385

Figure 16. The  $NH_3$  breakthrough measured as a function of  $\beta$  and  $T^*$  for three equivalence ratios.

appropriate conditions were provided. Calibration gases were detected and measured successfully, but the combustion product conditions are severely different from the cold flow calibration conditions. Rich combustion of the fuel oil to provide hydrocarbons in the product gas flow was not feasible due to reproducibility and stability problems arising from excessive flame length and sooting. To simulate combustion where hydrocarbons or hydrocarbon fragments are present, propane gas was injected into the combustion tunnel downstream of the visible fuel oil/air flame. Under these conditions, HCN was observed in the 1 to 10 ppm range, and four resolved peaks were detected on the gas chromatograph. Retention times and peak width were recorded, but no attempt was made to identify these compounds. Under normal conditions these peaks were never observed.

B. Fuel Nitrogen: Pyridine

In order to simulate the effect of nitrogenous species commonly found in fuels, we have studied the reduction process when pyridine is added to the fuel oil as a prototype fuel nitrogen compound. The pyridine is added volumetrically and is thoroughly mixed with the oil prior to spraying the fuel into the combustion tunnel. While a constant amount of pyridine is added to the fuel, the resulting NO concentration,  $[NO]_i$ , changes as a function of temperature and equivalence ratio of the reacting mixture. This is due to the incomplete conversion of the fuel nitrogen to NO as it passes through the flame, and the production of NO by thermal NO reaction mechanisms. Complete conversion of the nitrogen in a 4.93% by volume pyridine in fuel oil mixture would result in an NO concentration of approximately 1200 ppm at an equivalence ratio of 0.89. Table V lists the conversion efficiencies measured at various temperatures and equivalence ratios. The conversion percentages are corrected for the thermal NO produced when the fuel oil alone is burned under the same combustion conditions. Since pyridine itself is a fuel, the equivalence ratio should be corrected for its presence. However, at the concentrations used in this study, the change in the equivalence ratio with pyridine is well within the experimental error in the ratio introduced by the uncertainties in the flow metering. The NO concentrations when no ammonia is added range from 495 to 590 ppm. All NO reduction data are normalized to the measured initial NO concentrations.

With the pyridine-doped fuel, no visible changes were observed in the flame, or in the measured temperatures. However, low concentrations

TABLE V

## Conversion of Pyridine to NO

$\phi$	T*		[NO] <sub>i</sub> <sup>a</sup>	%
	mV	Corrected	ppm	Conversion to NO <sup>b</sup>
0.78	33.8	1103	545 - 555	42
	34.7	1128	560 - 565	43
	36.0	1147	570 - 575	44
	36.8	1170	580 - 585	45
	37.7	1197	580 - 585	45
	38.6	1224	585 - 590	46
0.89	37.0	1176	570 - 580	45
	37.4	1188	560 - 580	44
	37.5	1191	565 - 575	44
	37.7	1197	570 - 580	45
	38.0	1206	565 - 580	44
	38.2	1212	565 - 580	44
	38.3	1215	575 - 590	45
	39.8	1261	560 - 590	44
0.95	37.2	1182	530 - 540	41
	37.6	1194	540 - 550	42
	38.7	1227	540 - 550	42
	39.5	1252	530 - 540	41
	40.6	1289	530 - 545	41
	41.3	1315	515 - 535	40

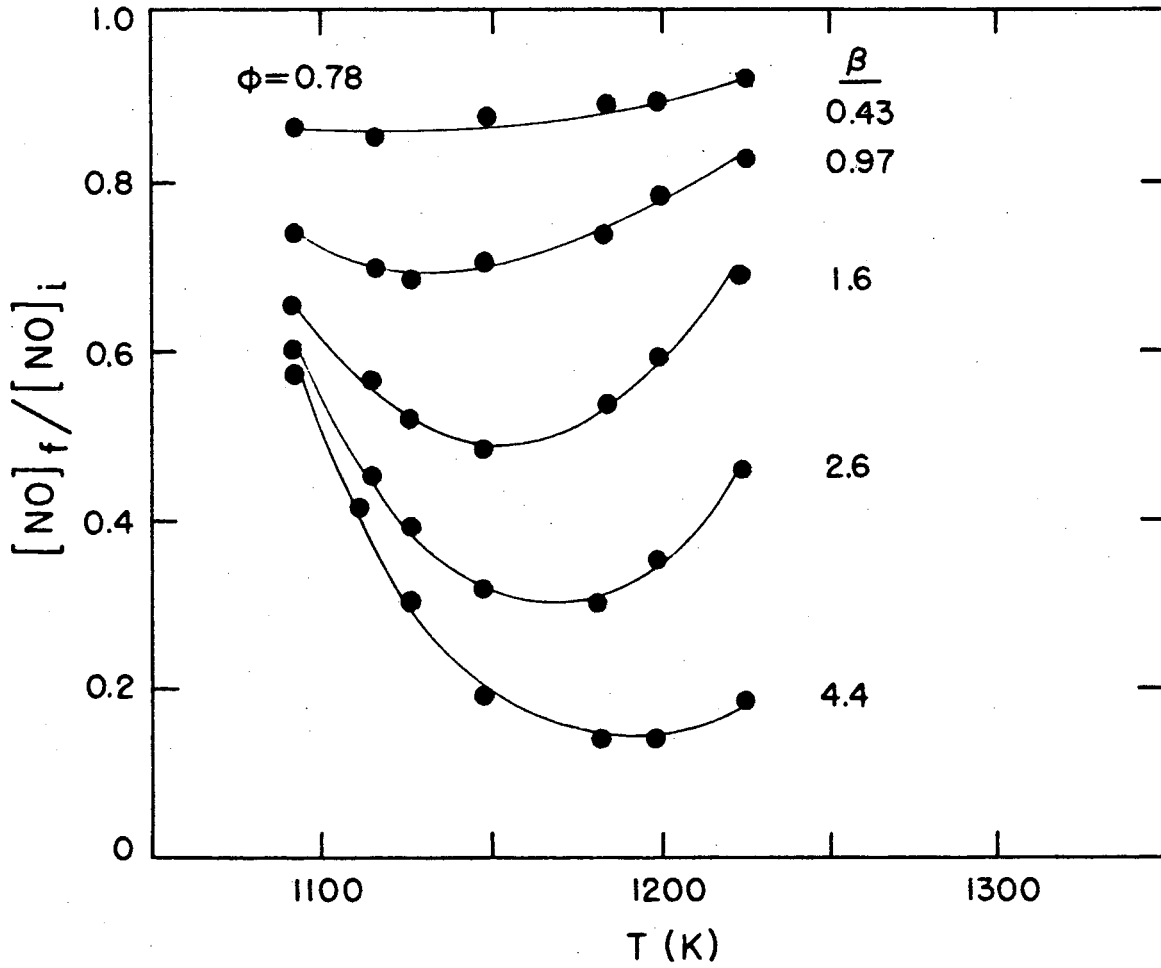
a) measured at final probe station

b) thermal NO is subtracted when calculating conversion efficiencies

of an oxidizable nitrogen compound were observed in the NO chemiluminescent analyzer when the samples were passed over the stainless steel catalyst. Measured values were typically  $5 \pm 5$  ppm. Because the measured concentration is a difference between the NO concentration and the NO plus oxidizable nitrogen compounds concentration, there is large uncertainty in the measured value which is estimated to be as large as the measured value itself. No  $\text{NH}_3$  or HCN could be detected by the other methods employed, indicating that the observed species is most probably  $\text{NO}_2$ .

The temperature dependence of the reduction process is shown in Figures 17, 18 and 19 for equivalence ratios of 0.78, 0.89, and 0.94. These measurements essentially duplicate the conditions studied when NO was used as the fuel nitrogen compound. The results of the ammonia addition on the reduction process are substantially the same as described previously. The extent of NO reduction, and optimum reaction conditions are not significantly different for the two different fuel nitrogen compounds. It is important to note, however, that the more extensive data for the pyridine doped fuel case permits greater precision in determining the optimum reduction conditions.

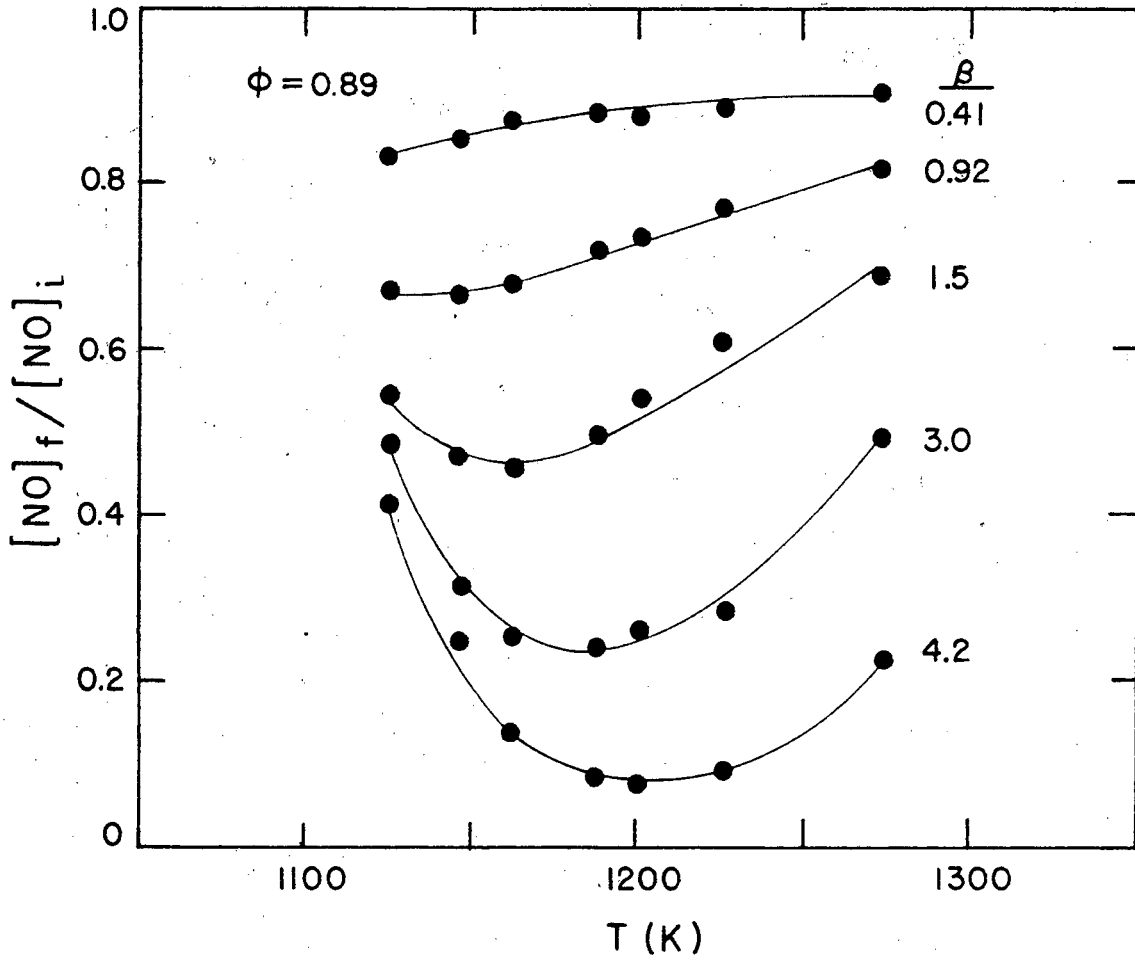
A portion of the ammonia breakthrough results are presented in Figure 20. These results are for the three different equivalence ratios at approximately the same  $\beta$  values (4.2 - 4.4). The measurements, made over a month long period of time and with the three different measurement techniques, illustrate the agreement and the estimated uncertainties in the measured quantities. These results are in good agreement with the ammonia breakthrough measurements presented in the previous section, again indicating that the type of fuel nitrogen compound used does not



XBL 812-8266

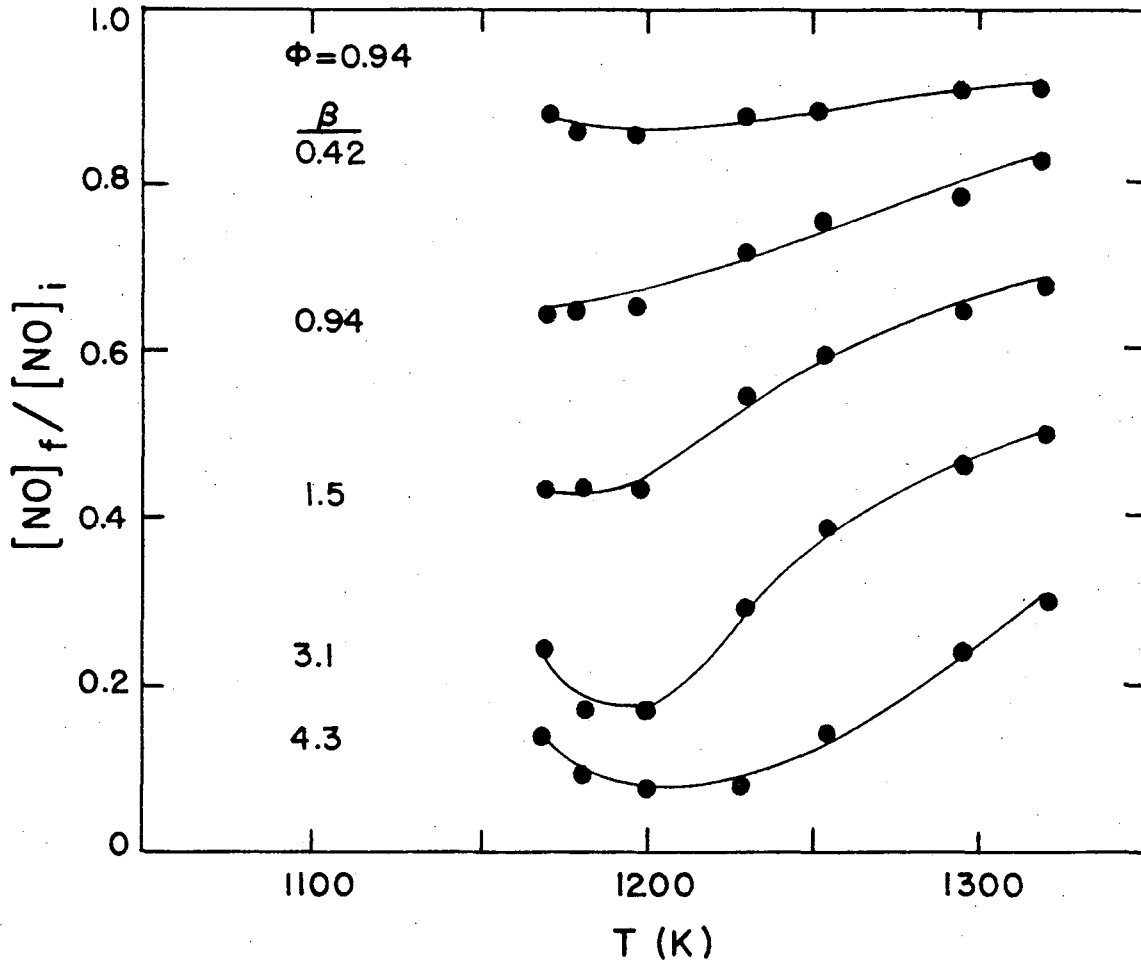
Figure 17. The NO survival as a function of  $\beta$  and  $T^*$  for  $\phi = 0.78$  with pyridine as the fuel nitrogen (1.02% N).





XBL 812-8279

Figure 18. The NO survival as a function of  $\beta$  and  $T^*$  for  $\phi = 0.89$  with pyridine as the fuel nitrogen (1.02% N).



XBL 814-9260

Figure 19. The NO survival as a function of  $\beta$  and  $T^*$  for  $\phi = 0.94$  with pyridine as the fuel nitrogen (1.02% N).

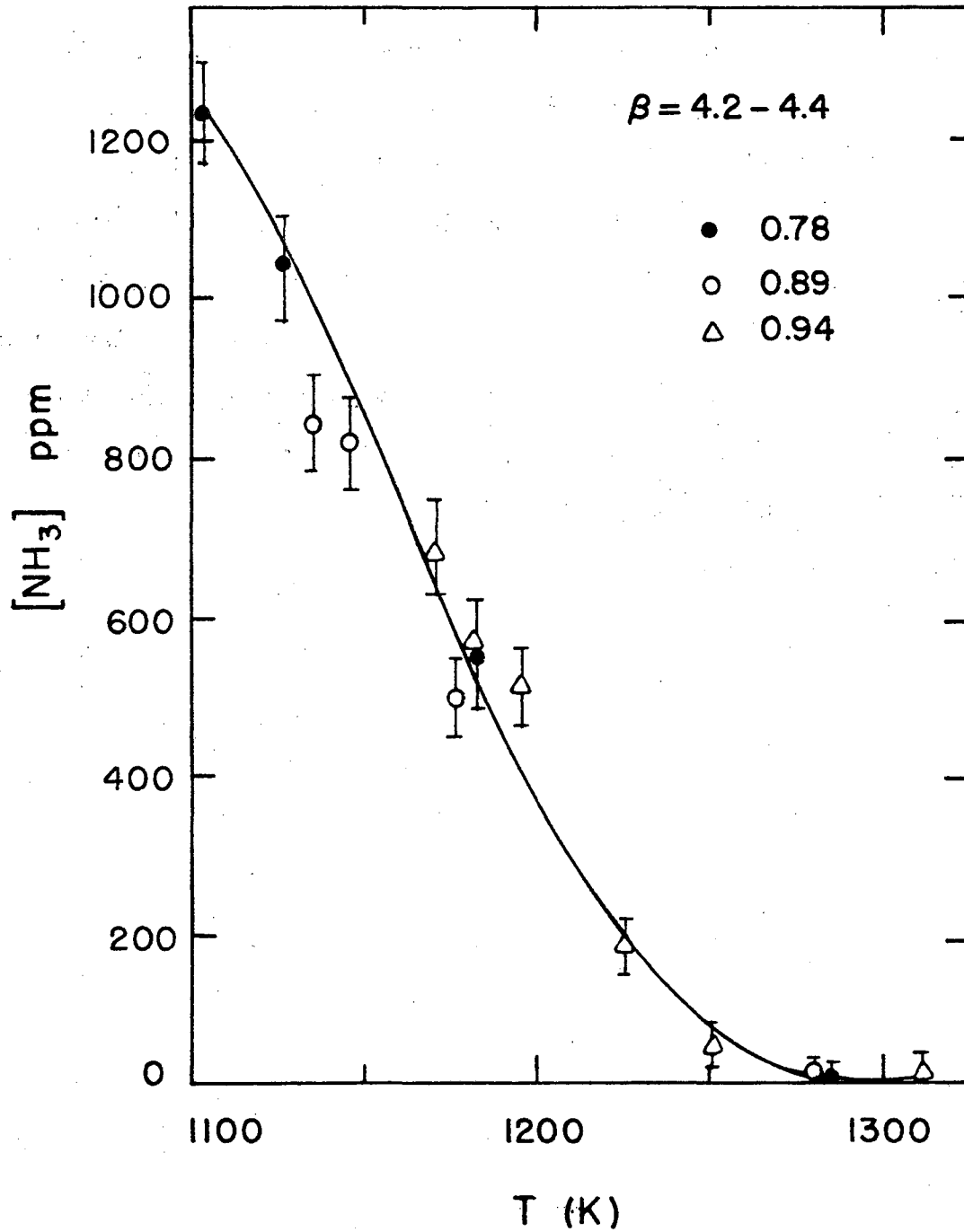


Figure 20. The NH<sub>3</sub> breakthrough measured as a function of T\* for three different equivalence ratios at  $\beta = 4.2 - 4.4$ .

effect the reduction process for lean combustion, and that the  $\text{NH}_3$  breakthrough is independent of the equivalence ratio.

Numerous attempts were again made to measure the presence of any other nitrogenous species. Apart from the small concentrations of the compound presumed to be  $\text{NO}_2$  that were observed and discussed previously, no measurable quantities of these other "odd nitrogen" species were detected for the range of experimental conditions studied. The agreement between the results using  $\text{NO}$  or pyridine as the fuel nitrogen species is strong evidence that no significant quantities of unobserved nitrogenous species are generated when pyridine is admixed with the fuel oil and then burned. Consistent with our other results, no hydrocarbons were observed in the combustion exhaust product gases.

C. Fuel Nitrogen: Pyridine                      Fuel Sulfur: Thiophene

Research concerned with the effect of sulfur chemistry on the selective reduction process has been inconclusive, and in general relatively little research effort has been directed toward investigating the coupling between nitrogen and sulfur combustion chemistry.

Since many fossil and synthetic fuels have substantial amounts of both fuel nitrogen and fuel sulfur, we have simulated these fuels by admixing both pyridine and thiophene with the fuel oil. Both compounds are added volumetrically to the fuel oil and are thoroughly mixed before combustion. Selected samples are withdrawn from the fuel supply for elemental analysis.

For this part of the study the equivalence ratio was fixed at 0.89, and the amount of pyridine added was constant at 1.02% fuel N (by weight). Prior to determining the effect of fuel sulfur on the  $\text{NH}_3$  reduction process, the conversion of fuel nitrogen to NO was measured as a function of fuel sulfur concentration. Table VI lists these results for three different fuel sulfur concentrations and various  $T^*$  values. With no pyridine or thiophene added to the fuel, thermal NO concentrations of 40-45 ppm were measured. The thermal concentration was subtracted from the  $[\text{NO}]_1$  values when calculating the fuel nitrogen conversion efficiency. The addition of fuel sulfur tends to increase the amount of NO formed from a fixed amount of fuel nitrogen. At a constant fuel sulfur concentration there is only a weak  $T^*$  dependence on the fuel nitrogen conversion. Measured  $\text{SO}_2$  concentrations indicate that within experimental error, quantitative conversion of the fuel sulfur to  $\text{SO}_2$  occurs when no  $\text{NH}_3$  is present. However, when both sulfur compounds and  $\text{NH}_3$  are present, serious errors occur in the measurements of both species due to the formation of

TABLE VI

## Conversion of Pyridine to NO

$\frac{T^*}{K}$	$\frac{\text{FUEL S}^a}{\%}$	$\frac{[\text{SO}_2]_i^b}{\text{ppm}}$	$\frac{[\text{NO}]_i^c}{\text{ppm}}$	$\frac{\% \text{ FUEL N}}{\text{CONVERSION TO NO}}$
1170±5	0.04	—	515±10	40
1188			510	39
1224			520	40
1252			515	40
1282			515	40
1176±5	0.33	148±15	600±10	48
1200			600	47
1230			615	48
1268			627	49
1293			650	51
1167±5	0.63		675±15	53
1194			670	53
1245			705	55

a) added as thiophene

b) measured at terminal probe station with no  $\text{NH}_3$  addition

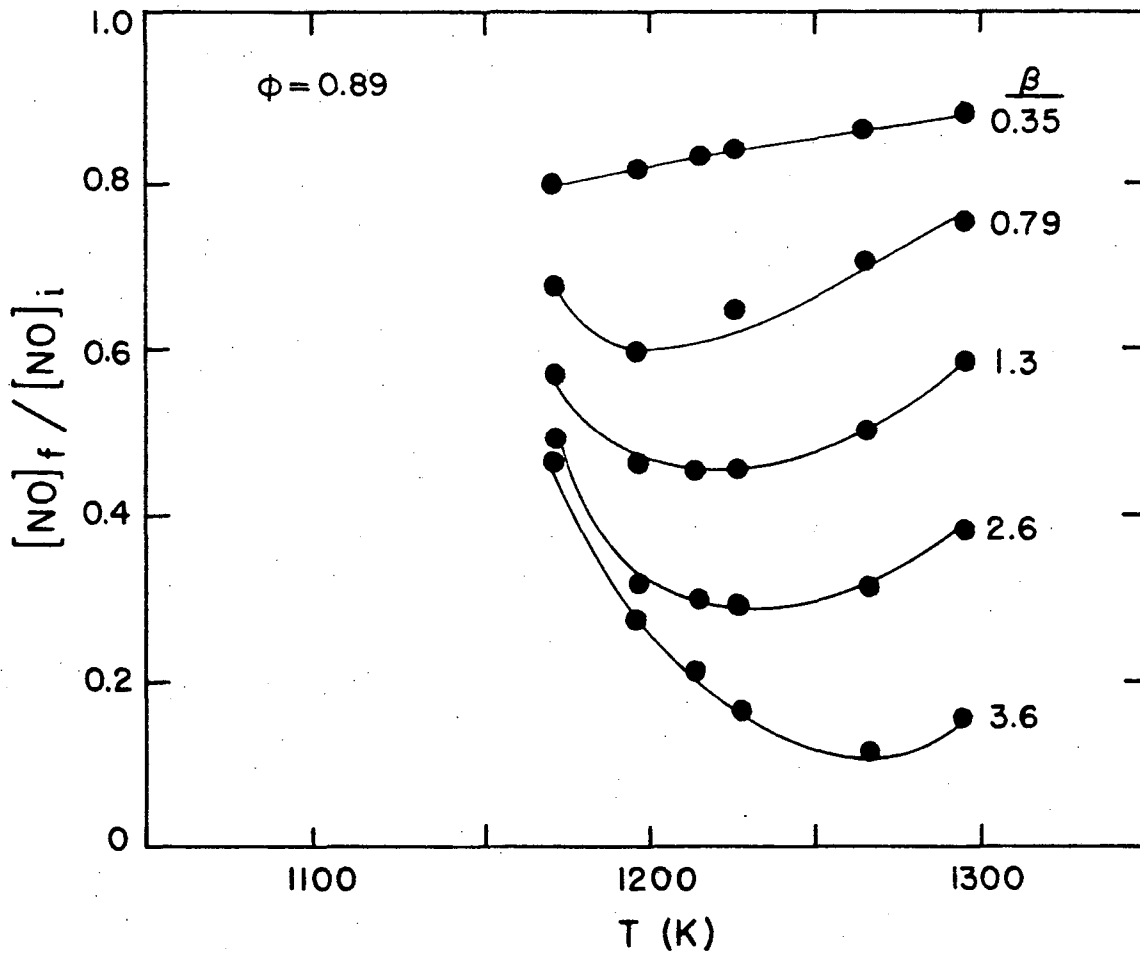
c) added as pyridine (1.02% fuel N)

sulfur-ammonia species.

The sulfur-ammonia compounds (ammonium bisulfate and similar species) decompose at the high temperatures in the reaction section, and are stable only at the lower temperatures found in the probes, sampling lines, or analyzers. The ammonium salts form as crystalline solids, which are in general very soluble in water.

The temperature dependence of the reduction process when thiophene is added to the fuel is shown in Figures 21 and 22. Figure 18 should also be examined, as these measurements were made at the same equivalence ratio and concentration of pyridine, but with no added thiophene. There is a noticeable shift to higher optimum reduction temperatures when the concentration of fuel sulfur increases. However, the maximum NO reduction for a fixed  $\beta$  value is not significantly altered at the optimum temperature, and the width of the temperature window for reaction is essentially unchanged though it is shifted to a higher temperature. A plot of NO reduction as a function of  $\beta$  at one fixed temperature is shown in Figure 23. At  $\beta$  values less than 1, the fuel sulfur appears to have little measurable effect on the NO reduction. Above  $\beta \approx 1$ , the change in the process at a constant temperature with increasing fuel sulfur is obvious. Preliminary results indicate that this trend continues at even higher fuel sulfur concentrations.

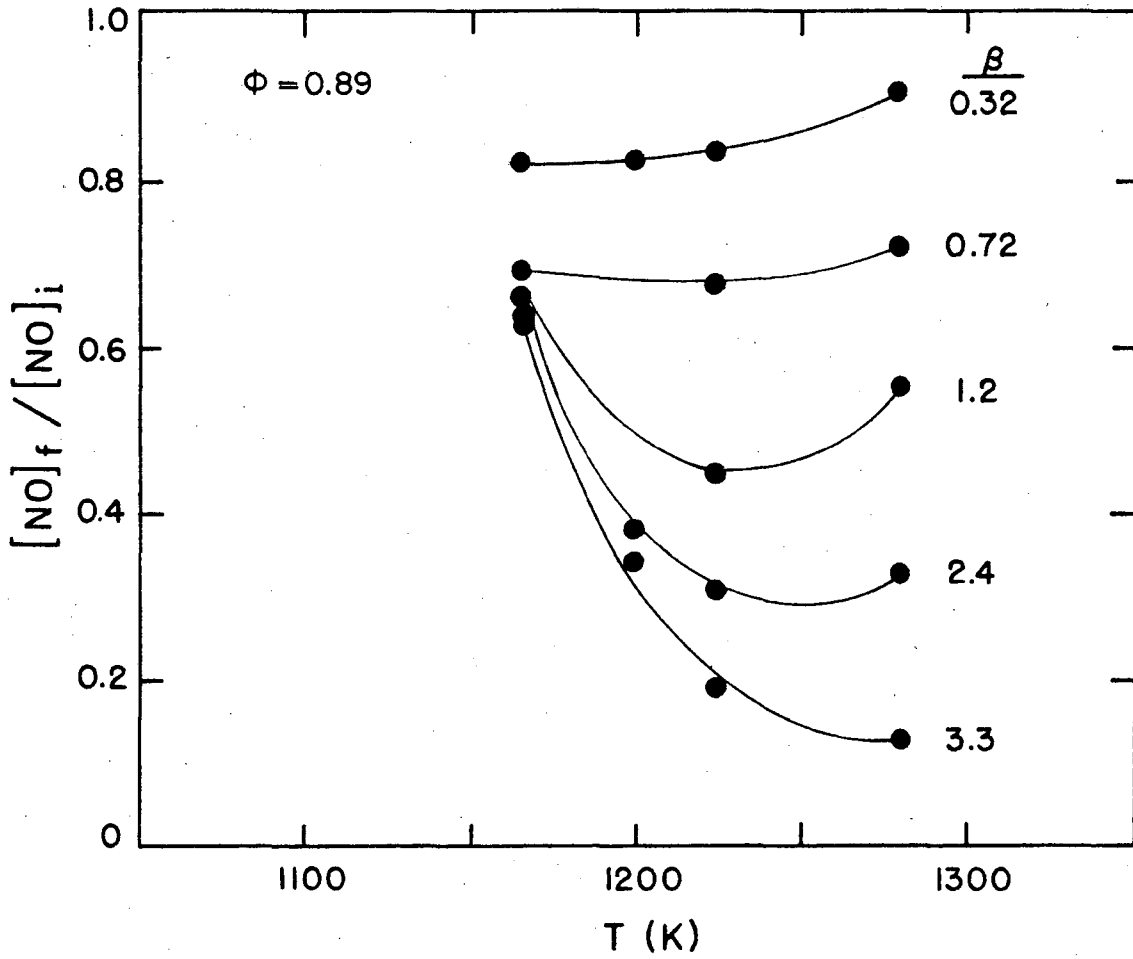
Accurate ammonia breakthrough measurements cannot be made because of the condensation of a white crystalline substance (presumably  $\text{NH}_4\text{HSO}_4$ ) in the sampling lines and in the chemiluminescent analyzer. The sodium phenolate method can be used to measure the total ammonia ( $\text{NH}_3$ ) and ammonium ( $\text{NH}_4^+$ ) species concentration, but further modifications of the sampling manifold are necessary to maintain a higher temperature throughout the sampling lines to prevent solids from depositing. Suitable techniques



XBL 812-8277

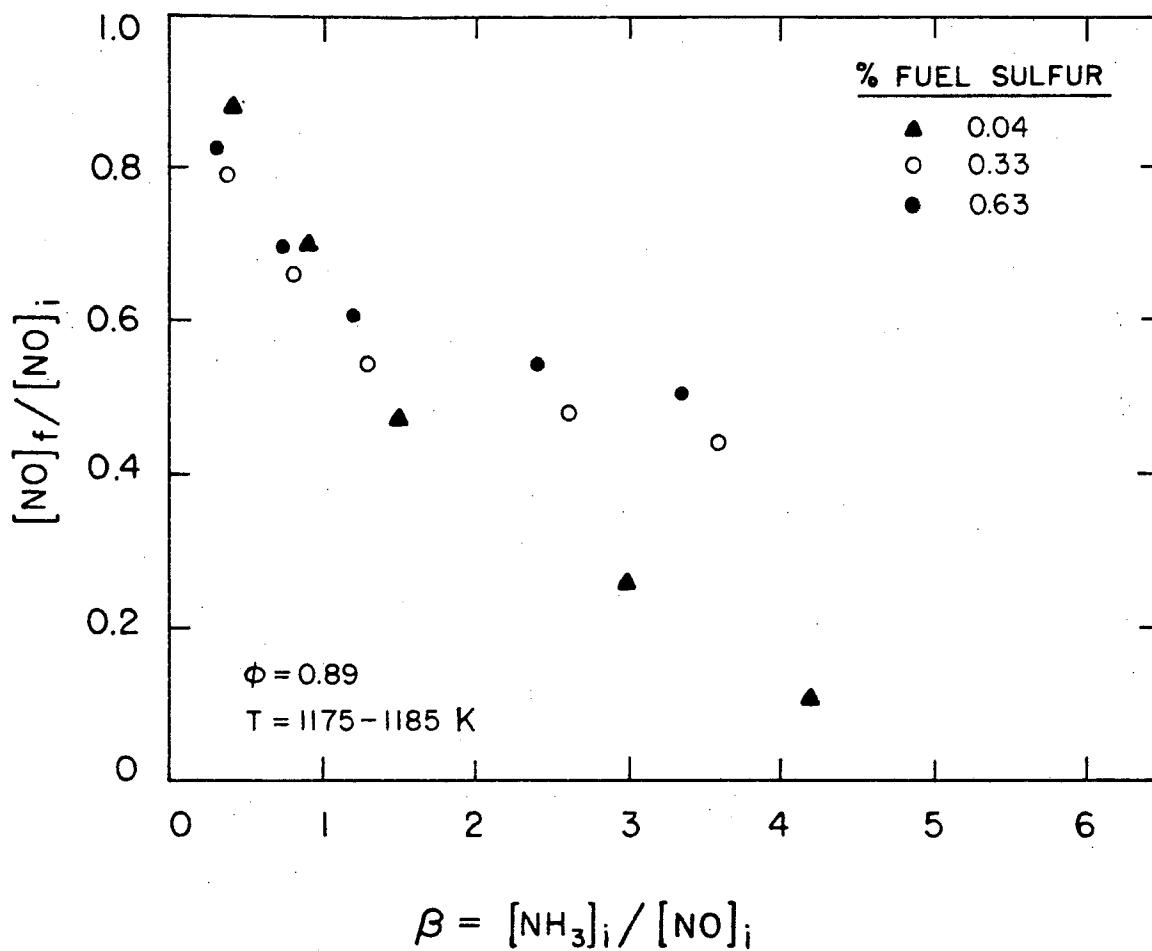
Figure 21. The NO survival as a function of  $\beta$  and  $T^*$  for  $\phi = 0.89$  with pyridine as the fuel nitrogen (1.02% N) and thiophene as the fuel sulfur (0.33%S).





XBL 812-8278

Figure 22. The NO survival as a function of  $\beta$  and  $T^*$  for  $\phi = 0.89$  with pyridine as the fuel nitrogen (1.02% N) and thiophene as the fuel sulfur (0.63% S).



XBL 812-8280

Figure 23. The NO survival as a function of  $\beta$  and fuel sulfur concentration for  $\phi = 0.89$  and  $T^* = 1175 - 1185$  K.

for measuring other nitrogenous species in the presence of both  $\text{SO}_2$  and  $\text{NH}_3$  will need to be developed to reduce the interferences that plague the present methods.

## V. DISCUSSION

The reduction of NO by NH<sub>3</sub> addition has been studied over a range of temperatures, equivalence ratios, amounts of NH<sub>3</sub> injected, and types and concentrations of fuel nitrogen and fuel sulfur. One of the most important results of this study is the absence of appreciable concentrations of nitrogenous species other than NO, NO<sub>2</sub>, N<sub>2</sub>, and NH<sub>3</sub> when the reduction occurs under lean conditions. A conservative upper limit for the total concentration of these "odd nitrogen" species is 5 ppm. We set this limit based on the absence of compounds measured directly by techniques such as GC, GC/MS, and wet chemical methods which are sensitive to nitrogenous compounds, and the agreement between the different analytical techniques used to measure NO, NO<sub>x</sub>, and NH<sub>3</sub>. As the different methods employed have widely different interferences, an appreciable concentration of an unobserved "odd nitrogen" compound could be detected as a difference in the measured concentration of NO<sub>x</sub> or NH<sub>3</sub>. Nitrogen compounds that are most certainly absent include HCN, nitriles, and amines; other more complex species are even less likely to be present. The absence of hydrocarbons or H<sub>2</sub> in the exhaust gases corroborates these results. Other researchers have reported similar findings. Lyon and Longwell found no evidence for HCN unless hydrocarbons were present in their flow reactor study, and Muzio, et al. found no HCN generated when NH<sub>3</sub> was introduced into the exhaust gases of a coal-fired combustor.

The extent of the NO reduction and the optimum conditions measured are qualitatively in agreement with results obtained previously by Muzio, et al., but differ somewhat quantitatively. The differences reported in

the optimum temperatures (generally  $< 50\text{K}$ ) most probably reflect differences in experimental design (temperature gradients, size of combustor, residence time in the reaction zone), method of ammonia injection, and measurement and definition of the ammonia injection temperature ( $T^*$  in this study). In addition, the observed dependence of the optimum temperature on  $\beta$  and the equivalence ratio can also partially account for the discrepancies.

The differences in the extent of the NO reduction for a given set of conditions is more puzzling. Muzio, et al, and Lyon and Longwell report greater reduction of NO for a given  $\beta$  at the optimum temperature than we observe. However, the coal-fired experiments and commercial installations of the Thermal DeNO<sub>x</sub> process have not achieved as deep reductions as in these previous laboratory studies. There are also some differences in the levels of NH<sub>3</sub> breakthrough reported by Muzio, et al.

We have examined our results to determine if a cause for these differences can be established. The possibility that the reaction is incomplete in our apparatus due to the 40 msec residence time, as compared with generally longer reaction times ( $\sim 50\text{ msec} - 1\text{ sec}$ ) in the other experiments, has been discounted by measurements such as those shown in Figures 9 and 10. These results are for reduction near the optimum temperature, and show that the reaction is essentially complete by the final probe station, and indicate that little further reaction can be expected for longer reaction times. At higher temperatures, oxidation of NH<sub>3</sub> increases as the temperature rises, leaving little NH<sub>3</sub> remaining to react (Figure 16). At lower than optimum temperatures, the reaction presumably slows sufficiently to prevent significant reduction even with longer residence times. Of course, a real or laboratory scale

combustor has both radial and axial temperature gradients which tend to reduce the temperature of the reactants as they flow through the combustor. Comparison of our apparatus to Muzio's indicate that we have smaller thermal gradients and finer control over the reaction conditions. While these conditions do not explain the NO reduction results, they, and our definition of  $T^*$ , can account for our  $\text{NH}_3$  breakthrough results which are consistently lower at a given temperature than Muzio's. Both studies indicate that as the temperature is lowered, all of the injected ammonia that does not react can be recovered. At higher temperatures, uncertainties in the measurement techniques, definition of the reported temperatures, and possible reaction on or in probes make direct comparisons difficult at this time. Further investigation into the measurement and probing techniques could aid in resolving this problem.

It is difficult to compare our results directly with Lyon's experimental studies or the theoretical studies which have modelled the reduction reaction for several reasons. They have used the nearly isothermal conditions of a plug flow reactor, and do not account for all of the species present in the combustion exhausts. In addition, they use fully equilibrated initial conditions, while our CO measurements approximately 40 ppm higher than expected from thermodynamic calculations suggest that the free radical concentrations in our apparatus may also be higher than expected, resulting in a faster observed reaction rate than seen by Lyon or calculated in the modelling studies.

The method of ammonia injection in our apparatus was extensively studied, with the conclusion that rapid and complete mixing was indeed occurring. Reaction of the ammonia as it passes through the injector system, yielding a lower concentration of ammonia than calculated, was

also considered, but previous experimental measurements showed that no reaction occurred in  $\text{NH}_3 - \text{N}_2$  mixtures when passed through hot quartz tubing similar to the injectors. Probe and wall effects are much more difficult to determine. Catalytic effects of metal probes or platinum thermocouples could enhance the reaction or destruction of  $\text{NH}_3$ , or quartz sampling probes could cause oxidation of the  $\text{NH}_3$  to NO. Further and more careful study into the effects of many of these possibilities may lead to a more complete understanding of their role in the reduction reactions.

The presence of fuel sulfur has two different, though interrelated manifestations: there is an increase in the conversion of fuel nitrogen to NO as the fuel is burned, and the optimum temperature for the  $\text{NH}_3$  reduction process shifts to higher values. The observed increase in NO production in the presence of fuel sulfur is in agreement with the results of Wendt et al.<sup>24</sup> Wendt et al. added  $\text{SO}_2$  or thiophene to fuels doped with  $\text{NH}_3$  or pyridine, and showed that the burning characteristics of the fuel were not affected by the addition of an aromatic fuel but rather by the presence of organic sulfur by doping the fuel with benzene in place of thiophene. They reported NO produced to be quite dependent on the method of mixing the fuel and air. It is very difficult, however, to quantitatively characterize "mixing" in a turbulent diffusion flame. In our study, the flow conditions were held constant and there were no visible differences in the flames when thiophene was present. Since we have made no attempt to observe reaction intermediates during the combustion of fuel nitrogen, we can only speculate as to the cause of the increased NO formation.

The dependence of the selective reduction of NO by  $\text{NH}_3$  on

temperature and  $\beta$  has been discussed previously. Sulfur compounds in the post-combustion gases could affect the reduction process by reacting with the ammonia or an ammonia derived species, effectively lowering the concentration of the reducing agent (lower  $\beta$ ). This would result in less NO reduction and in a decrease in the temperature for achieving the optimum NO reduction. Neither of these is observed. Lower concentration of  $\text{SO}_2$  and  $\text{NH}_3$  are measured when both species are present, but this is most likely attributable to reactions in the sampling system. The observed shift in the optimum temperature suggests a change in the reaction mechanism, or the presence of a competing reaction pathway when sulfur compounds are present. Sulfur dioxide has been identified as the major product of sulfur compounds in lean combustion environments; however, other sulfur compounds present in significantly smaller concentrations could also be important. Muzio, et al. in their coal study, did report a significant variation in the optimum reduction temperature for different fuels, but did not explain these results. They did study the addition of  $\text{CS}_2$  to the fuel supply of a fuel oil/air mixture and found no significant difference in the reduction process. The coal with the highest optimum temperature did have the highest fuel sulfur concentration, however. Additional research is warranted to further ascertain the role of various sulfur compounds in nitrogen combustion chemistry.



## VI. SIGNIFICANCE TO LARGE SCALE APPLICATIONS

The control of oxides of nitrogen emissions from large stationary combustion sources has been primarily based on combustion modification. The first applications of combustion modification for oxides of nitrogen control in electric utility boilers were undertaken more than 25 years ago. Combustion modification methods have proven particularly effective for gas fired units, but less so for oil and coal fired furnaces and boilers as a result of higher fuel nitrogen levels in the liquid and solid fuels and added difficulties in controlling mixing processes. Post combustion NO<sub>x</sub> control methods are now being explored and, in some cases, large scale applications have or are being demonstrated.

Post combustion methods are generally divided into two types: wet or dry<sup>25</sup>. Of these approaches the dry methods, based on selective catalytic reduction (SCR) or selective non-catalytic reduction (SNR) appear currently to be the most promising. Both methods have been applied commercially to large scale units in Japan<sup>26</sup>. The SCR methods have the potential for reductions in NO concentrations of up to 90% or greater but appear to suffer catalyst contamination problems. The SNR methods utilizing NH<sub>3</sub> showed the potential for 80-90% reduction in laboratory tests but have, somewhat disappointingly, yielded reductions of only 50% or less in early field applications. Due to the sensitivity of the SNR methods to temperature, the variability of gas temperature at the point of ammonia injection with unit load appears to be the major difficulty. Overcoming this difficulty would require changing the injection location with load, the use of a temperature

window shifting additive, e.g. hydrogen, and/or sophisticated temperature and composition sensing and ammonia flow control to optimize the process for changing loads and NO levels.

The major potential environmental consequence of ammonia addition for NO<sub>x</sub> control is the breakthrough of ammonia. In common with the temperature sensitivity of the reduction of NO<sub>x</sub>, the breakthrough of ammonia is also sensitive to temperature. Only at temperatures in excess of those which are optimum for NO<sub>x</sub> control do ammonia levels approach zero. Again, the control of ammonia emissions requires a generally not provided ability to control ammonia flow rates both in magnitude and location of injection in response to conditions at the point of injection.

Extrapolation of laboratory studies to large scale applications is difficult because of the disparity in residence times-- on the order of 100 milliseconds or less in these experiments in comparison with five to ten times greater residence times in large installations. However, since 35 msec appear adequate to reach a steady state at the optimum temperature for the Thermal DeNO<sub>x</sub> process (about 1230 K), the disparity in residence times between laboratory and full scale experiments will be important only at off-operating conditions.

An important parameter affecting both NO removal and ammonia breakthrough is the cooling rate of the combustion gases, that is, the rate of temperature decrease. In utility applications this parameter is fixed by heat exchanger and flow characteristics and is not readily controllable. The performance of the Thermal DeNO<sub>x</sub> process, consequently, is likely to be installation specific. Monitoring of NO and

and  $\text{NH}_3$  is, therefore, essential for optimization of the process for both maximum NO removal and minimum  $\text{NH}_3$  breakthrough. Since some trade-off between NO and  $\text{NH}_3$  emissions appear inherent to the Thermal DeNO<sub>x</sub> process (greater injection rates of  $\text{NH}_3$  generally lead to lower NO but higher  $\text{NH}_3$  emissions) some basis for assessing an acceptable or optimal combination of the emissions is required. Such information is not currently available since the role of  $\text{NH}_3$  as an air pollutant is not well understood. Possible atmospheric interconversions or synergistic effects are similarly poorly defined subject topics.

Attempts to identify other secondary pollutants associated with the Thermal DeNO<sub>x</sub> process have failed to identify potential problems. This is consistent with other investigations. While absolute confirmation that no such problems exist is not possible, this study contributes to a growing body of information suggestive that major problems of secondary pollution formation are unlikely.

The present study has provided new information on the interaction of sulfur with the Thermal DeNO<sub>x</sub> process which suggest that fuels with high sulfur levels will require a reoptimization of conditions for the application of ammonia for oxides of nitrogen control. High sulfur fuels may result in the lowering of ammonia breakthrough (either because of higher optimum injection point temperatures or because of the formation of ammonium bisulfate), but concurrently create other problems such as deposits in air preheaters and corrosive attack. The presence of sulfur compounds (primarily  $\text{SO}_2$  and  $\text{SO}_3$ ) in exhaust gases make measurements of ammonia by extractive methods extremely difficult. Consequently, all measurements of ammonia breakthrough for applications involving high sulfur

fuels (perhaps as little as 0.1% fuel sulfur) are suspect and probably unrealistically low.

The Thermal DeNO<sub>x</sub> process provides effective NO<sub>x</sub> control technology which is likely to see large scale application. Optimization of NO removal and minimization of NH<sub>3</sub> breakthrough requires a greater degree of monitoring and process control than is being employed on current installations and may prove cost effective and environmentally desirable.

REFERENCES

1. Lyon, R.K., U.S. Patent No. 3,900,554, August 1975.
2. Lyon, R.K. and Longwell, J.P., EPRI NO<sub>x</sub> Control Technology Seminar, San Francisco, CA, 1976.
3. Lyon, R.K., Int. J. Chem. Kin., 8, 315, 1976.
4. Lyon, R.K. and Benn, D.J., Seventeenth Symposium (International) on Combustion, 601-610, 1979.
5. Lyon, R.K., Hardy, J.E. and Benn, D.J., Paper No. WSS/CI 78-51, presented at the Fall Meeting of the Western States Section of The Combustion Institute, 1978.
6. Muzio, L.J., Arand, J.K. and Teixeira, D.P., Sixteenth Symposium (International) on Combustion, 199-208, 1977.
7. Muzio, L.J., Arand, J.K. and Maloney, K.L., Report No. KVB-15500-717B, 1978.
8. Saliman, S. and Hanson, R.K. Combustion Science and Technology, 23, 225, 1980.
9. Miller, J.A., Branch, M.C., Kee, R.J. To be published in Combustion and Flame, 1981.
10. Banna, S.M., and Branch, M.C., Paper No. WSS/CI 78-50, presented at the Fall Meeting of the Western States Section of The Combustion Institute, 1978.
11. Lewis, P.F., Brogan, T., Johnson, D.M., Stevens, F.M., and Kothandaraman, G. Paper presented at the Fall Meeting of the Eastern States Section of The Combustion Institute, 1980.
12. EPA/IERL-RTP Report No. EPA-600/7-79-079, March 1979.
13. EPA/IERL-RTP Report No. EPA-600/7-79-111, May 1979.
14. Brown, N.J., Sawyer, R.F., and Eitzen, T.S. Report to the California Air Resources Board, 1979.
15. Basden, K.A., private communication.
16. Colket III, M.B., Chiappetta, L.J., Zabielski, M.F., Seery, D.J., Guile, R.N., and Dodge, L.G. To be published in the Eighteenth Symposium (International) on Combustion, 1981.
17. Matthews, R.D., Sawyer, R.F., and Schefer, R.W., Environmental Science and Technology, 11, 1092, 1977.

18. D. Lucas, A.S. Newton, K. Metchette, and N.J. Brown (in preparation)
19. E. Cuellar, private communication.
20. Myerson, A.L. Fifteenth Symposium (International) on Combustion 1085, 1975.
21. Starkman, E.S. Combustion Generated Air Pollution. Plenum Press, New York, 1971.
22. Analyses were performed by the Microchemical Analysis Laboratory, University of California, Berkeley.
23. Silver, J.A., and Kolb, C.E. Chem. Phys. Lett. 75, 1, 191, 1980.
24. Wendt, J.O., Morcomb, J.T. and Corley, T.L., Seventeenth Symposium (International) on Combustion, 671-678, 1979.
25. EPRI Report No. FP-1109-SR, July 1979.
26. EPA/IERL-RTP Report No. EPA-600/7-79-205, August 1979.

LIST OF ABBREVIATIONS AND SYMBOLS

A, B, C, D	- - - - -	probe and thermocouple axial positions
$\beta$	- - - - -	ratio of $\text{NH}_3$ added to initial NO concentration
CL	- - - - -	centerline
CLA	- - - - -	chemiluminescent analyzer
GC	- - - - -	gas chromatography
GC/MS	- - - - -	gas chromatography/mass spectrometry
NDIR	- - - - -	non-dispersive infrared
$\phi$	- - - - -	equivalence ratio
SCR	- - - - -	selective catalytic reduction
SNR	- - - - -	selective non-catalytic reduction
$T^*$	- - - - -	temperature at ammonia injection site
[ ]	- - - - -	denotes species concentration

Subscripts

i	- - - - -	initial value
f	- - - - -	final value

50272-101

<b>REPORT DOCUMENTATION PAGE</b>	<b>1. REPORT NO.</b> LBL-12549	<b>2.</b>	<b>3. Recipient's Accession No.</b>						
<b>4. Title and Subtitle</b> The Selective Reduction of NO through Ammonia Addition		<b>5. Report Date</b> July 1981							
<b>7. Author(s)</b> N.J. Brown, R.F. Sawyer, and D. Lucas		<b>8. Performing Organization Rept. No.</b> LBL-12549							
<b>9. Performing Organization Name and Address</b> Energy and Environment Division Lawrence Berkeley Laboratory University of California Berkeley, CA 94720		<b>10. Project/Task/Work Unit No.</b>  <b>11. Contract(C) or Grant(G) No.</b> (C) A8-146-31 (G)							
<b>12. Sponsoring Organization Name and Address</b> Air Resources Board State of California P.O. Box 2815 Sacramento, CA 95812		<b>13. Type of Report &amp; Period Covered</b> Final 7/20/79 to 1/31/81 <b>14.</b>							
<b>15. Supplementary Notes</b>									
<b>16. Abstract (Limit: 200 words)</b>  The selective reduction of NO by NH <sub>3</sub> addition has been studied in a lean-burning oil fired laboratory combustion tunnel as a function of equivalence ratio, NH <sub>3</sub> injection temperature, concentration of NH <sub>3</sub> added, and the source of NO. Ammonia breakthrough was found to depend strongly on the NH <sub>3</sub> addition temperature. The total concentration of nitrogen containing species other than N <sub>2</sub> , NO, and NH <sub>3</sub> was measured with a variety of techniques and was found to be less than 5 ppm over the range of conditions studied.									
<b>17. Document Analysis</b> <table border="0" style="width: 100%;"> <tr> <td style="width: 15%;"><b>a. Descriptors</b></td> <td>Pollution, NO Formation, Selective Non-catalytic reduction</td> </tr> <tr> <td><b>b. Identifiers/Open-Ended Terms</b></td> <td>Thermal DeNO<sub>x</sub> NO<sub>x</sub> Reduction Pollution Abatement</td> </tr> <tr> <td><b>c. COSATI Field/Group</b></td> <td></td> </tr> </table>				<b>a. Descriptors</b>	Pollution, NO Formation, Selective Non-catalytic reduction	<b>b. Identifiers/Open-Ended Terms</b>	Thermal DeNO <sub>x</sub> NO <sub>x</sub> Reduction Pollution Abatement	<b>c. COSATI Field/Group</b>	
<b>a. Descriptors</b>	Pollution, NO Formation, Selective Non-catalytic reduction								
<b>b. Identifiers/Open-Ended Terms</b>	Thermal DeNO <sub>x</sub> NO <sub>x</sub> Reduction Pollution Abatement								
<b>c. COSATI Field/Group</b>									
<b>18. Availability Statement</b> Release Unlimited. Available from National Technical Information Service 5285 Port Royal Rd. Springfield, VA 22161		<b>19. Security Class (This Report)</b>	<b>21. No. of Pages</b>						
<b>20. Security Class (This Page)</b>		<b>22. Price</b>							



This report was done with support from the Department of Energy. Any conclusions or opinions expressed in this report represent solely those of the author(s) and not necessarily those of The Regents of the University of California, the Lawrence Berkeley Laboratory or the Department of Energy.

Reference to a company or product name does not imply approval or recommendation of the product by the University of California or the U.S. Department of Energy to the exclusion of others that may be suitable.

TECHNICAL INFORMATION DEPARTMENT  
LAWRENCE BERKELEY LABORATORY  
UNIVERSITY OF CALIFORNIA  
BERKELEY, CALIFORNIA 94720